Written Review of Informal Meeting on Impurity Control Toroidal Devices

A.T. Mense

April 1974

UWFDM-100

Written Review of Informal Meeting on Impurity Control Toroidal Devices

A.T. Mense

Fusion Technology Institute
University of Wisconsin
1500 Engineering Drive
Madison, WI 53706

http://fti.neep.wisc.edu

April 1974

UWFDM-100

Written Review of Informal Meeting on

Impurity Control Toroidal Devices

by

Allan T. Mense

April, 1974

Nuclear Engineering

University of Wisconsin

Madison, Wisconsin, 53706

FDM 100

The following paper is a review of the Informal Meeting on Impurity control in Toroidal Devices held by the A.E.C. on Oct. 31, 1973 at Philadelphia, Penn.

This review was composed and edited by the author and only recently distributed to the meeting participants. The review is presented in as coherent yet straight forward a fashion as possible. It is hoped that this review may be of general interest and so is reproduced here as an F.D.M.

Participant List

K. Gentle
RLM 11.212
University of Texas
Austin, Texas, 78712

R. A. Gross
Columbia University
New York, N.Y. 10027

J. T. Hogan, C. F. Barnett
Oak Ridge Nat'l Lab.
P.O. Box Y
Oak Ridge, Tenn   37830

A. L. Hunt, R. W. Moir
L - 386
Lawrence Livermore Lab.
P.O. Box 808
Livermore, Calif. 94550

G. A. Emmert, A. T. Mense
Nuclear Engineering Dept.
1500 Johnson Drive
University of Wiscons-n
Madison, Wisconsin 53706

R. P. Madden
A 251, Physics Bldg.
National Bureau of Standards
Washington, D. C. 20234

E. Apgar
Rm. 26-231
MIT Research Lab. of Electronics
Cambridge, Mass. 02142

F. H. Tenney
U. R. Christensen
S. Gralnick   } Princeton
E. Hinnov   Plasma Physics
D. Meade   Laboratory
H. Furth   Box 451
                    Princeton, N.J.
                              08540

D. M. Gruen
Chemistry Division
Argonne National Lab.
9700 S. Cass Ave.
Argonne, Ill.   60439
                    } Argonne
M. Kaminsky
Physics Division
Argonne Nat'l Lab.
9700 S. Cass Ave.
Argonne, Ill.   60439

T. Oliphant
Las Alamos Scientific Lab.
Las Alamos, New Mexico   87544

W. Bauer
Sandia Laboratories
Livermore, California   94550

T. Tamano
Gulf General Atomics Co.
P.O. Box 608
San Diego, Calif.

D. Ignat (CTR)
K. M. Zwilsky (CTR, D&T) } USAEC
Wm. C. Gough (CTR)
F. R. Scott (CTR)

Review on Impurity Control Meeting

by A. T. Mense

In present day Tokamaks, energy loss is through several mechanisms. Ion heat conduction predominates in the central core region, with energy loss due to charge exchange neutrals and line (free-bound and bound-bound) radiation contributing significantly towards the edge. (Another edge loss mechanism is of course particle loss to the limiter if the plasma is in contact with it. Some of the charge exchange neutrals produced hit the chamber walls and release either cold fuel atoms or sputter off wall material. The ST results tend to show that the impurity metal content of the plasma increases slowly as the discharge proceeds in time. These energy loss mechanisms are present in both ORMAK and ST. While there appeared during the course of the meeting to be some controversy between ST and ORMAK, John Hogan has indicated that this is not really so that the ratio of (charge exchange/line radiation) energy loss is not an issue. There is some difference of opinion however about this ratio for _future_ experiments. Included in appendix A are a number of graphs furnished by John Hogan explicating the points be addressed. A complete discussion of the charge exchange bombardment problem as discussed at the meeting by John is written up in ORNL-TM-4474 entitled "Fluxes, of Charged and Neutral Particles from a Tokamak", by Hogan and Clarke. A couple of reports concerning ST results are MATT-852 on "Particle and Energy Balance in the ST Tokamak" by Dimrock, et.al., and MATT-973 on "Princeton Tokamak Experiments", by H. Furth.

Dale Meade (PPL & U. of Wisc) discussed the impurity problems in present day Tokamaks and extrapolated some information on impurity effects on ignition conditions for future reactor concepts. He noted

that if an impurity gets completely stripped of its electrons (as oxygen does in ST) and migrates to the center of the discharge it essentially does no further damage from the energy balance point of view. This is because it is then only susceptible to classical Bremsstrahlung radiation which is negligible in present day Tokamaks (due to $T_e \sim 1$ KeV) but would not necessarily be negligible in fusion reactors. ($T_e \sim 10$ KeV). Metal impurities (Fe, W, Mo, Au) are another story. These atoms only become partially stripped and effect the energy balance primarily due to recombination (free-bound) radiation which is important at both high and low T_e if Z is large enough.

The topic of "effective Z" was brought up at this point. Dr. E. Hinnov has furnished a good explaination of this topic:

"The effective ion charge $\bar{Z}$ for Coulomb collisions is

$$\bar{Z} = \frac{\sum_i Z_i^2 N_i}{\sum_i Z_i N_i}$$

in a plasma with ions in different charge-states i. However, if the atoms retain some bound electrons, as the heavier elements normally do, this definition is ambiguous. Thus, for free-free bremsstrahlung, especially at the shorter wavelength Z_i should be nuclear charge or perhaps nuclear charge minus two (for K-electrons), whereas for recombination radiation and plasma resistivity Z_i is the net charge (although electron-electron interaction with the bound electrons may also be significant). It is mainly for this reason that the quoted "effective Z" for the same plasma may vary over considerable range, depending on the method of measurement.

[Another, quite artificial ambiguity arose from the fact that some people have defined "effective Z" as the ratio of measured resistivity to Spitzer resistivity of pure hydrogen plasma. Actually,

of course, Spitzer resistivity increases less rapidly than linearly with $\bar{Z}$, because the relative contribution of (free) electron-electron interaction decreases with increasing $\bar{Z}$.]"

It was indicated that there was good reason to believe that if one could "encourage" the discharge to strike in the volume of the chamber, as opposed to at the limiter, that this metal impurity problem could be reduced. Also the use of a low Z limiter may be called for if one indeed is going to use a physical (not magnetic) limiter in future experiments (Ref. MATT-989 by D. Meade)

Questions were raised as to whether or not a poloidal divertor would alleviate the start up impurity content problem because of its dependence on the plasma current to provide a separatrix. In this vain also there was some concern as to whether or not impurities could be ionized in the divertor zone "soon enough" during the start up phase to be of value in lowering the "effective Z" of the plasma. Gil Emmert (U. of Wisc.) noted that one may have to consider a toroidal or a "bundle" divertor for the start up phase but it would probably be an expensive way to go. (It is noted that in a conceptual Tokamak fusion reactor such as UWMAK-I the poloidal divertor magnet costs are comparable to the toroidal magnet costs anyway.) The impression was made that many of these problems could be alleviated if one knew how to "lay in" the current profile for the Tokamak discharge. Some attempt will be made to do this in PLT.

Sam Gralnick (PPPL) introduced another problem which one will encounter when extrapolating present day devices into a reactor regime and his findings indicate that impurities will be even more of a problem if one insists on using predominatly ohmic heating. The essence of his argument is as follows.

If one uses ohmic heating ($\therefore T_e > T_i$ by necessity) then the power/volume introduced into the plasma equals ηJ^2. Now η has a density dependence only in a log term and therefore consider it density independent as a first approximation. From MHD stability considerations, (kink modes) one finds that the stability margin at the plasma "edge" is $q(a) \gtrsim 2$, where

$$q(a) = \frac{a}{R} \frac{B_T}{B_P} = \frac{2B_T}{\mu_0 R} \frac{1}{J}$$

and for simplicity, J is taken constant for illustrative purposes. The other quantities are;

$\qquad$ a = plasma (minor) radius

$\qquad$ R = torus (major) radius

$\qquad$ B_T = Toroidal field

$\qquad$ J = current density

For economically concievable* Fusion Reactors with $B_T \sim 30 - 50$ KG and $R \sim 10 - 15$ m (ref. Matt-973 by H. Furth) one finds $J \approx 30 - 50$ amps/cm^2 [one notes that ORMAK and ST have $J \approx 100-150$ amps/cm^2 and PLT will have $J \approx 250$ amps/cm^2]. Thus one will be faced in larger scale reactors with a reduced ohmic heating power/vol. to balance out impurity radiation effects. Even though the surface to volume ratio of the torus is smaller as one approaches the reactor regime it may not decrease enough to compensate for the reduced ηJ^2. One conceptual solution was mentioned for large reactor startup. That is the possibility of using ohmic heating to heat up a smaller volumed, low density ($n < 10^{12}$cm^{-3}) plasma over a period of tems of seconds (time scale limited by power supply capabilities) and thus achieve T_{ign}. Then

---

*As of 1973 Studies ($P \approx 5000$ MW$_{th}$)

one could go into a density build up and volume expansion phase using auxilliary forms of heating (and fueling). Whether one could do this and maintain MHD equilibrium and stability is unknown at this time. Even if neutral beam heating provides a suitable supplementary heat source it may still be worth while to investigate the concept of low density, small volume start up. Remember that after T = Tignition then one has α's to help in heating which is by far the strongest energy source available for that purpose.

Before discussing the edge temperature problem, there were several points introduced in the meeting which were glossed over but yet are of import in my opinion. First, to my knowledge, no one has shown theoretically (or experimentally) that a Tokamak plasma which has a null in the poloidal field at its boundary (defining if you will its "boundary") can be MHD <u>stable</u>. Indeed <u>at the nulls</u> $\nabla\psi = 0$ and the MHD equilibrium equations indicate one cannot contain a plasma there. Obviously the "boundary" will be a little bit inside the separatrix. It seems that only experimentally will we be able to tell what a "little bit" is. Secondly, in the poloidal divertor designs to date, (UWMAK-I, PPPL conceptual design, PDX) it appears that plasma in at least some part, if not all, of the divertor region (outside the separatrix) is in a zone of unfavorable curvature and thus susceptible to flute or ballooning MHD modes. Possibly the electron mobility along the field lines to the collectors will be large enough so that "line trying", may prevent these modes from growing. Thirdly, it should be noted that steep density and maybe steep temperature gradients (and impurity gradients) may be present near the separatrix between the plasma core and divertor zones. These gradients lead to drift type insta-

bilities which tend to scale like Bohm ($D \sim \frac{1}{B}$) in terms of their effect on the diffusion of particles across the fields. One may however be able to live with Bohm type cross field diffusion if it is not too high.

These gradients should also open the divertor up into all the mirror instabilities. These instabilities should keep the loss core filled and may significantly reduce the number of particles mirror trapped in the outer divertor zones. If one tends to rely on a "mirror" trapped divertor plasma to ionize wall originated (high Z) impurities then these mirror instabilities are dileterious to that cause.

There was considerable discussion during the meeting of what mechanisms would be responsible for energy transport at the plasma edge and thus determine, through the energy and flux of charge exchange neutrals, the severity of the sputtering problem on the first wall of a fusion reactor. The conversations were complicated by the inter-change of information on several different concepts all at the same time. It may best be separated into the following concerns.

First, in present day devices the edge temperature is determined to a great extent by impurity line radiation and charge exchange. The electron-ion equilibration time for a hydrogen plasma

$$\tau_{equil}^{e-i} \cong 1.66 \times 10^{12} \, \frac{(T_{kev}^{e})^{3/2}}{N(\#/cm^{3})} \, \frac{1}{\ln\Lambda} \quad sec.$$

is a few milliseconds or so for these devices. Therefore, any mechanism which tends to lower Te also effects Ti and visa-versa. Electron energy of course is pumped up by ohmic heating fields. Charge exchange of protons on impurities is negligible as is classical Bremstrablung and synchrotron radiation.

As one proceeds to next generation devices, Dale Meade indicates
that preliminary calculations on a poloidal devertor device (PDX) tend
to show that the edge temperature may never be able to exceed about
200eV. His calculations are based upon the classical electron thermal
conductivity along the field lines in the divertor zone to the particle
collectors. These results are still priliminary however, Dale has
recently allowed his estimates to creep up.

Obviously if the charge exchange rate is substantial then the plasma
temperature profile can only be found by solving the particle and energy
balance equations selfconsistently (simultaneously). These equations
are non-linear integro-differential equations and can present problems
even for computer analyses. If one finds the edge temperature for the
plasma to be on the order of 100 eV or so this does not alleviate the
sputtering problem for the first wall. The logic is as follows.
Suppose one must loose 6 KeV in one (central) energy confinement time
in order to achieve an energy balance. If the edge temperature were
found to be high, and presuming the controlling mechanism was still
charge exchange, one might loose this energy as two 3 KeV neutrals let
us say. These two 3 KeV neutrals do a certain amount of sputtering
damage on the first wall. If instead of a high edge temperature, one
found that the edge temperature was lower, say 100 ev. Then to loose
this 6 KeV (still by charge exchange) one must do so through the loss of
sixty 100 eV neutrals. The sputtering coefficient for 100 eV neutrals
is less than that for 3 KeV neutrals. The question settles around
how much the sputtering coefficient is reduced for 100 eV as compared
to 3 KeV neutrals. This is a function of many factors [A good short
review is given in the radiation damage section of the University of

Wisconsin report on their conceptual design of a Tokamak fusion

reactor (UWFDM #68, sec. VI-C-5, pg. VI-C-47 to VI-C-65, Nuclear Engr.

Dept., Univ. of Wisconsin, Madison)]. I personally looked at several

references and found that it was not unusual for the sputtering

coefficient $S(3KeV) \gtrsim 100 \; S(100eV)$. If sputtering of wall atoms was

the only consequence of having 3 KeV neutrals hit the wall, then one

sees that,

$$2(3 \text{ KeV n's}) \times S(3 \text{ KeV}) \gtrsim 60 \times S(100eV) = 60 \times \frac{S(3KeV)}{100} = .6 \times S(3 \text{ KeV})$$

so the conclusion might be that going to lower edge temperature is

not of benefit unless T at the edge is reduced to $\theta(20eV)$ where $S \sim 10^{-4}$

or less.

While one can catch the gist of the argument, one can equally

well wonder whether or not different edge temperatures might not re-

flect completely different (dominating) physical transport mechanism

present in the divertor region. Depending on the divertor collector

capture effeciency and neutral reflux rate to the plasma edge, it

may be possible to "burn out" the neutral density in the divertor

zone (to less than $10^{10} \; cm^{-3}$) so that charge exchange effects will

be negligible.

It should be remembered here that the only fueling mechanism

present in these and even next generation devices is that of having

"cold fuel" at the edge. Beams will be used for heating not fueling

therefore charge exchange problems should continue to be with experi-

ments for a while.

Before moving on to more of the materials and surface physics

problems, there was a question posed by Ralph Moir (LLL) concerning

whether or not the plasma, inside and/or outside the separatrix, would take on some net charge?

Since no answer was given during the meeting, Ralph Moir drafted a restatement of the problem and a partial reply thereto. Appendix F reproduces his letter.

Surface Physics

In the area of surface physics, the problems which were addressed were 1) surface damage due to charged particles, neutrons and photons, and 2) divertor collector efficiency for D & T.

Treating the second of these points first, Dr. D. M. Gruen (Argonne) addressed the problem of chemically trapping D and T in the divertor in order to achieve the necessary pumpout rates. He showed quantitative results based upon particle fluxes calculated for the Princeton conceptual design of a Tokamak fusion reactor. (Appendix B contains a copy of a paper he presented at Argonne.) Essentially, he indicated that 95% of D & T leaving through the divertor could be collected by chemical trapping. This corresponds to having to process 2 tons of metallic hydrides per day of reactor operation in a 5000 MW_{th} plant assuming 4% burn up of D, T. This does not constitute any major chamical engineering problem.

In another vien, Dr. Gruen was asked what effect using C as a wall material would have. He indicated that if one goes to a low Z wall or limiter material such as carbon, that has a low physical sputtering coefficient, one must still be concerned with chemical sputtering. Hydrogen and carbon can form volatile hydrides such as methane which could cause severe sputtering. No quantitative information was detailed however.

Bob Gross (Columbia University) presented several slides showing the damage produced on a polished stainless steel surface when it was brought in "contact" with a warm plasma (Ti ~ 500-600 eV, N_i ~ $2 \times 10^{16} cm^{-3}$) whose magnetic field is parallel to the plasma-wall interface.

Unfortunately Dr. Gross's talk was missed by my tapes of that evening. Fortunately however one of his graduate students, Dr. Ben Feinberg, who performed much of this work has sent a copy of a paper covering just this topic. This paper is reproduced in Appendix C.

Still in the context of charged particle surface damage, Walter Bauer (Sandia, Livermore) and Manfred Kaminsky (Argonne) both presented helium blistering data and Kaminsky also showed D^+ blistering data and some recent experimental findings as to 14 MeV neutron sputtering effects. Before detailing this, a short note on surface damage effects in general is warranted in order that one might summarize and understand the data presented. I paraphrase part of a University of Wisconsin FDM - #68.

Due to the fluxes of charged particles, neutrons, neutral atoms, and gamma rays incident on the first wall, many primary and secondary interaction processes will occur which can 1) result in the degradation of mechanical properties of the wall and 2) produce an effective erosion of the wall material. Primary reactions may be defined as those interactions between the incident ion and the target where a momentum transfer occurs, a change in the internal energy state of one or both particles occurs, or when a nuclear reaction takes place. The result of these reactions is that secondary reactions such as lattice atom displacement, or ionization and x-ray emission may occur. Such processes can cause a variety of phenomena—physical and chemical sputtering,

blistering, secondary electron emission, x-ray emission, backscattering

of particles and photons, release of absorbed gases, radiation damage,

photodecomposition of surface compounds, particle entrapment and re-emission

of trapped particles.

The above processes have been studied but not necessarily in the

environments characteristic of fusion devices. Sputtering and

blistering appear, however, to be the most significant of these

processes in terms of wall integrity and imputity control.

Sputtering: the phenomena whereby atoms are ejected from the

lattice only by momentum transfers in the collision process is termed

physical sputtering. Data for low energy light ions on metals is

difficult to measure and also difficult to find in the literature.

Physical sputtering can, however, basically be understood by analyzing

the individual collisions of the incident ion and its primary knock-on

atoms (PKA's) in the lattice. The displaced atoms all slow down by

undergoing further collisions in the lattice. As this occurs, they

may diffuse and escape. Also, collisions beneath the surface may

result in focusing events which transfer monentum along close-packed

rows of atoms. If these close packed rows terminate on the surface,

enough energy might be imparted to the atom at the surface so that

it is ejected from the surface. Until the incident ions reach the

KeV region one may treat the collisions as essentially hard sphere

collisions. As a rule of thumb one may compute the threshold energy

for the onset of physical sputtering by noting that one must impart

about 5 eV of energy to a lattice atom to release it from the surface.

The average energy transfer to a PKA is given by

$$\overline{E}_{PKA} = \frac{E_{max}}{2} = 2 \frac{M_1 M_2}{(M_1 + M_2)^2} E_{ion}$$

for $M_1 = M_H$, $M_2 = M_{Fe}$ one has

$$\overline{E}_{PKA} \approx \frac{E_{ion}}{57} \overset{\geq}{=} 5 \text{ eV} \Rightarrow E^{ion}_{threshold} \approx 285 \text{ eV}.$$

So that <u>on the average</u> a 285 eV Hydrogen ion could provide sufficient

energy to sputter an Fe atom. The reason for the sputtering coefficient

rapidly rising in these low energy ranges is easily seen from this model

since $E_{pka} \propto (E_{ion})$ incident in this hard sphere collision regime.

[see fig. 1 enclosed].
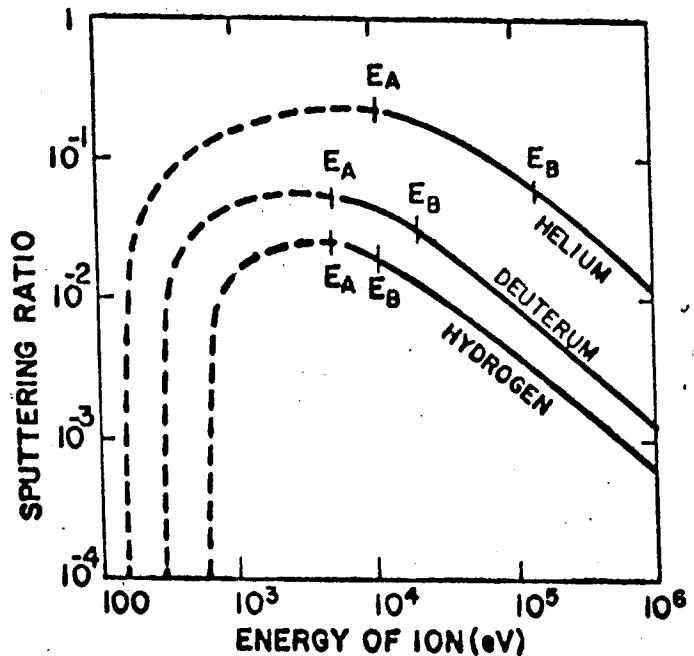
Figure 1   Calculated sputtering ratio of various
ions on silver, as a function of energy
The energy limits for weak screening
and hard sphere collision are E_B and E_A
respectively. The dashed portion of the
curves indicate regions of decreased relia-
bility. (76)

From FDM #68, U. of Wisc, Nuclear Engr. Dept.

To appear in J. Nucl Mati.
Aug. 74 issue
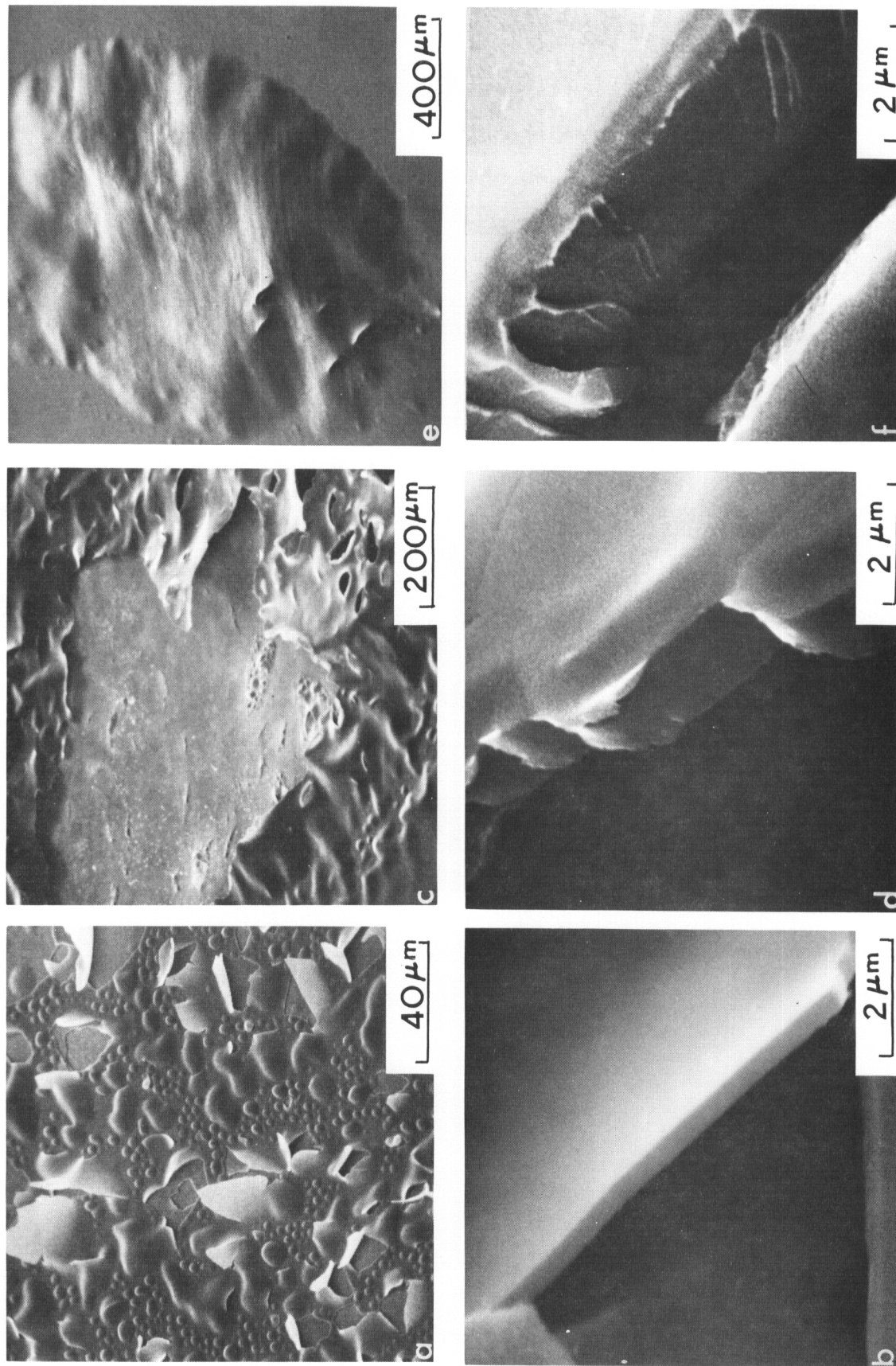
FIG 2

SEMs of polycrystalline niobium surfaces irradiated at room temperature (a) with 100-keV ^{4}He$^+$ ions to a total dose of 0.5 C/cm^2, (b) an enlarged view of the blister skin in (a), (c) with 0.5-MeV ^{4}He$^+$ ions to a dose of 1.0 C/cm^2, (d) an enlarged view of blister skin in (c), (e) with 1.5-MeV ^{4}He$^+$ ions to a dose of 1.0 C/cm^2 and (f) an enlarged view of the blister skin in (e).

Bauer and Thomas have studied the temperature dependence of He

reemission from 316 SS, Mb, Va, and Mo. (Ref. J. Nuc. Mat, <u>47</u>,

241 (1973). Their data on S.S. is what was presented by Walter

Bauer at this impurity meeting. (Appendix D) Kaminsky also pre-

sented some He blistering data in Nb and 304 S. Steel. [(Ref:

1) M. Kaminsky & S. K. Das Trans. Am. Nucl. Soc. <u>17</u>, 135 (1973),

2) S. K. Das & M. Kaminsky Nuc. Metallurgy <u>18</u>, 240 (1973), 3)

S. K. Das & M. Kaminsky, J. App. Phys. <u>44</u>, 25 (1973), 4) S. K.

Das & M. Kaminsky, IEEE Trans. Nucl. Sci, April (1974)].

Kaminsky observed that for the same total dose and target tem-

perature D - blistering is substantially less corrosive then He-

blistering (Ref: Rad. Effects <u>18</u>, 245 (1973).

Kaminsky's pictures of He blistering in annealed polycrystaline

Nb showed that 1) the thickness of blisters corresponded to the

range of the He ions in the metal (see Fig. #2) and 2) at higher

energies and therefore deeper penetration one expects the blister

area to be larger and his data confirms this. As sample tempera-

ture is increased to above half of melting point one starts to

anneal out nucleation centers for bubble formation and blister

formation (and size) decreases. (see Fig #3 & 4) These pictures

include effects of 100 KeV He on S.S. @ 450° C. As one changes the

angle of incidence of the beam from normal incidence to say 45°

one finds that foils (exfoliation) of material are produced.

Blistering: Qualitatively, energetic ions displace atoms as they pene-
trate the solid target. When they loose most of their energy, they
slow down and become trapped because of their low diffusivity. Since
the solubility of some of the gases in metals (e.g. helium) is very
small, most of the gas precipitates into small bubbles. These small
bubbles form near the end of the range for the gas atoms and this
region also corresponds with that for maximum vacancy production. The
bubbles can capture these vacancies, grow and eventually coalease with
other bubbles to form what are called lenticular bubbles below the
surface of the metal. If enough atoms are injected then depending on
the sample temperature, the pressure (nKT) in these bubbles will be
high enough to deform the metal surface causing it to protrude above
the original surface. Blister formation has been found to occur with
He bombardment but does occur to an extent with deuterium ion bombard-
ment in several materials (Noteably Nb, Mo, and stainless steel).

At the present time the size, density, shape and critical fluence
for the formation of blisters is found to be a function of at least
nine parameters:

1) Energy of ions (i.e. their range)

2) Diffusivity of injected ions

3) Solubility of gas atoms in matrix

4) Yield strength of the metal

5) Temperature of the metal during bombardment

6) The dose rate of bombarding ions

7) Total dose

8) The orientation of the crystal structure to the ion
   beam

9) The metallurgical state of the sample prior to irradiation,
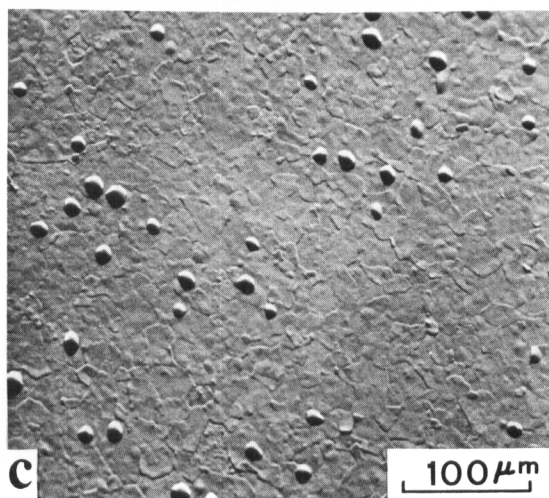   i.e. cold worked vs annealed.

ANNEALED POLYCRYSTALLINE VANADIUM IRRADIATED
WITH 0·5-MeV ^{4}He$^+$ TO A DOSE OF 1·0 C/cm^2
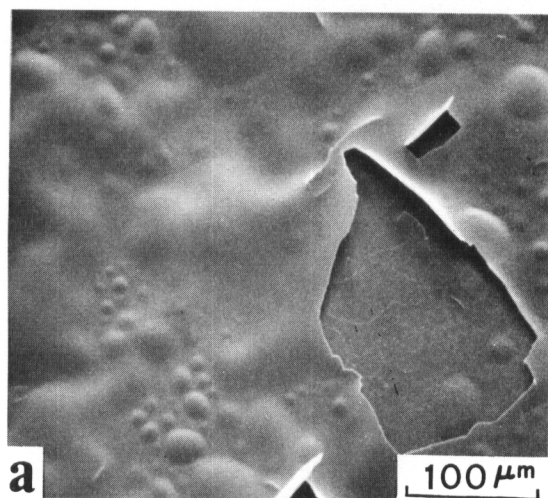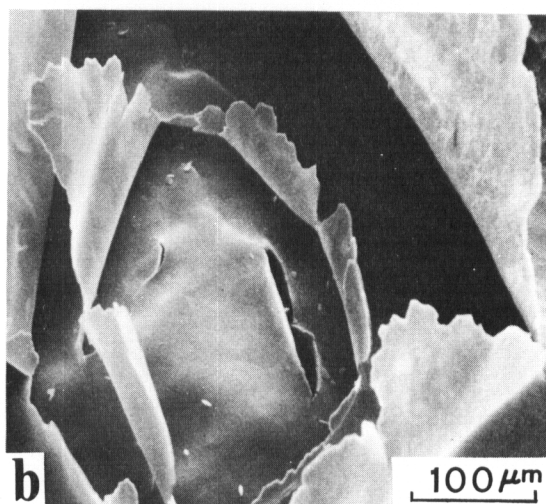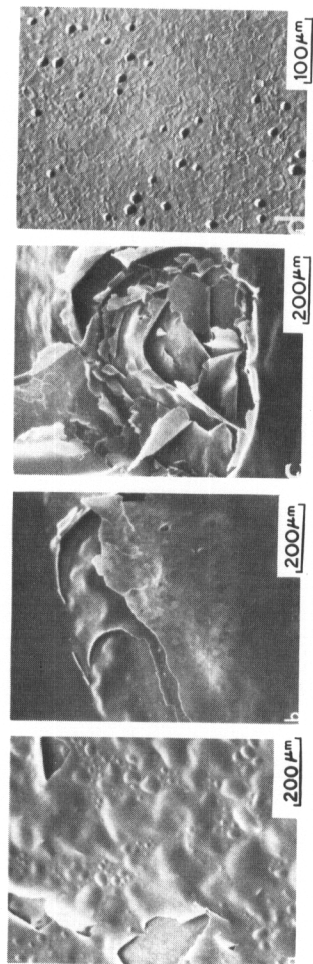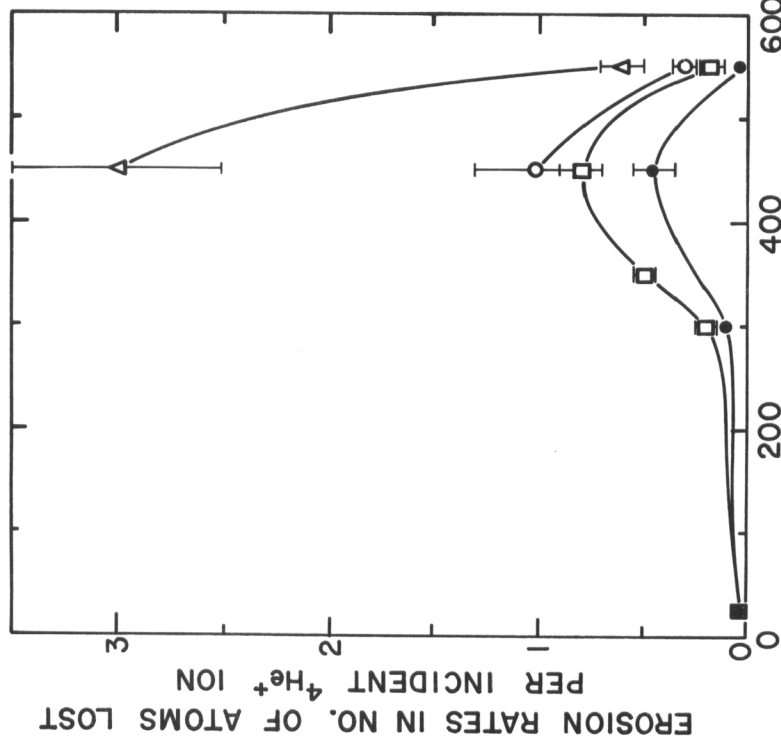

FIG. 3

Fig. 3 Scanning electron micrographs of annealed polycrystalline
vanadium surfaces after irradiation with 0.5-MeV ^{4}He$^+$ ions to a
total dose of 1.0 C/cm^2: (a) at room temperature, (b) at 600 ± 20°C,
(c) at 900 ± 20°C.

FIG. 4

(A) Erosion rates for annealed Type 304 stainless steel as a function of irradiation temperature for different projectile energies and total doses; ▪: 0.5 C/cm² with 0.5-MeV ⁴He⁺, □: 1.0 C/cm² with 0.5-MeV ⁴He⁺, ○: 0.1 C/cm² with 100-keV ⁴He⁺, ◁: 0.5 C/cm² with 100-keV ⁴He⁺. (B) Erosion rates for annealed polycrystalline vanadium as a function of irradiation temperature for 0.5-MeV ⁴He⁺ ions and for a total dose of 1.0 C/cm². The figures (a)-(d) at the top of Fig. (B) show SEMs of irradiated surfaces for the temperatures indicated therein.

Bauer's data (300 KeV He ions incident on S.S.) on He re-emission phenomena graphically and pictorially indicated that blister bursting was a significant re-emission effect so long as the sample temperature was not too high. [see Appendix D] The "incubation time" for blister formation before bursting agreed with simple ideal gas law pressume balances. His data indicated that above 600°C blisters ruptured (see Fig.5) after a total He doses of 5 x 10^{17} atoms/cm^2 of 300 KeV He ions. Bauer indicated that going to b.c.c. materials like vanadium would be better in terms of having a reduced blister bursting He re-emission rate [ref: Jour. Nucl. Mat. 47 (1973) 241]. A good short review of these effects is presented in MATT-1005 by Harolyn K. Perkins of Princeton.

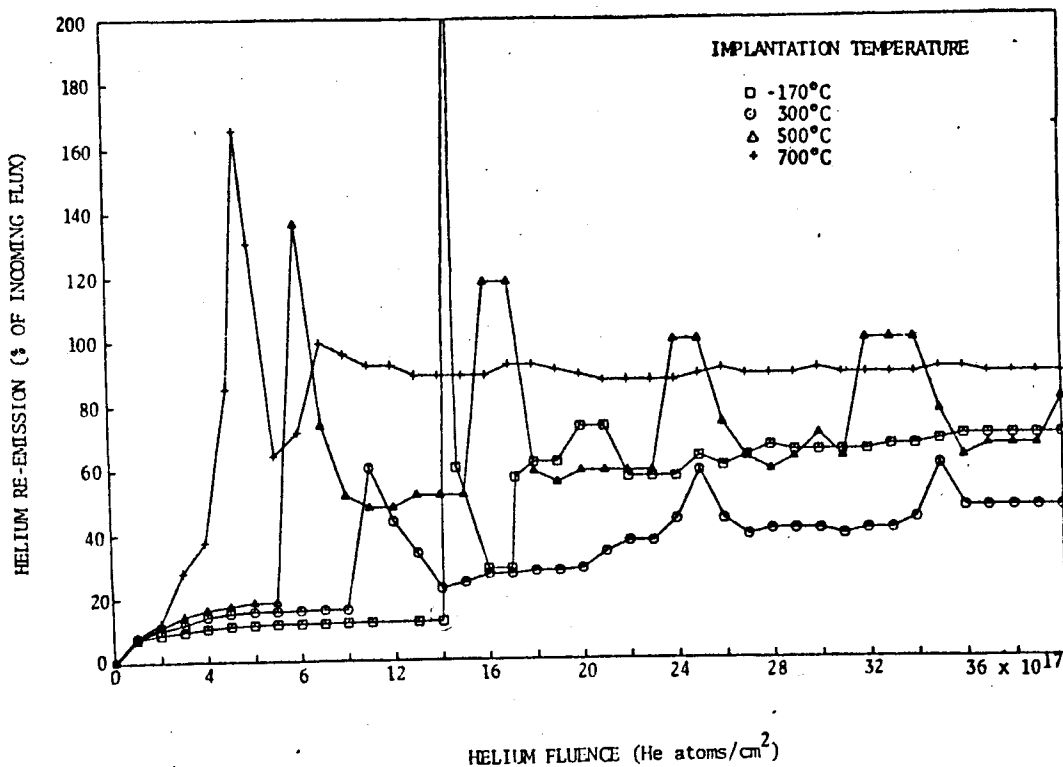*W. Bauer, G.J. Thomas, Surface deformation in 316 stainless steel*

Fig. 1. Helium re-emission during implantation as a function of helium fluence in 316 stainless steel at four different implantation temperatures.

Fig. 5

The topic of neutron sputtering due to 14 MeV neutrons was brought to light by the recent experimental investigations of Kaminsky (performed at LLL) (Ref: Bull. Am. Phys. Soc. 19, 31 (1974), Phys. Rev. Let. 32, 1599 (1974)). Kaminsky discovered the presence of "chunks" of sample material which had literally been expelled from the irradated sample. These "chunks" come off in both the incident direction of 14 MeV n's (i.e. out of back of sample) and also in the backward direction (i.e. from front of sample). In appendix E is a copy of a letter from Dr. Kaminsky on this matter as well as a reproduction of his Phys. Rev. letter.

Some recent theoretical work will soon be published regarding a possible mechanism for this "chunk" emission. It is the work of Dr. M. Guinan (LLL) and is entitled 'Shock Wave Interactions Arising from Near Surface Displacement Cascades'. It should appear in the Aug. '74 issue of J. of Nuclear Materials.

Bob Madden (Nat'l Bureau of Standards) expressed concern in two areas. One was the effect of secondary electron emission due to the high photon flux on the first wall. I would add here that ions and electrons can also cause secondary electron emission. The emissions of these secondary electrons could effect the energy transport and impurity transport in the divertor region. Bob's second concern was the possibility of vaporizing already ruptured blister or exfoliated material. As can be seen in Fig. #3 these thin foils are in poor thermal contact with the rest of the wall and concievably could be vaporized by an intense enough photon flux.

Kaminsky also noted that photon impact of energetic x and γ rays should be studied on insulators since power deposition can lead to

localized heating. This can cause high thermal gradients and thus stress gradients which can lead to spallation. (Ref. Kaminsky, Nuclear Metallurgy, Vol. 18,   ).

There were two topics also discussed in the meeting which did not conveniently fit into the above scheme of presentation.

Dr. Tom Oliphant (LASL) presented a review of his work on using a high density neutral gas blanket as a heat conduction method for the final cooling stages of a theta-pinch fusion reactor design. As Oliphant's work is presented in detail in Nuclear Fusion Vol. 13, 4 (1973), it is probably worthwhile only to mention his results. In essence he demonstrated that one could lower the temperature of a 6-10 KeV plasma down to the 1 eV range in reasonable distances with reasonable neutral densities and in reasonable times. The question which still has to be answered is whether or not one could inject suffient cold neutral gas into the vacuum region between the hot plasma and the wall carefully enough to avoid prohibitivly large charge exchange neutral fluxes to the wall.

Ralph Moir (LLL) presented a possible method of solving the divertor problem in a Tokamak. Although it is somewhat easier to visualize with a drawing (see Appendix F) his idea was to expand the poloidal divertor channel out into the low toroidal field region and possibly even beyond the "D" magnets. By collecting the particles in a low field (expanded magnetic flux) region one gains by lowering the energy density of the diverted plasma. Also since the cross field drift velocity is proportional to (kT/B), one notes that in low B regions one can have fairly high cross field transport rates so that the transit time to the particle collectors may be shorter than one

would anticipate assuming the particles had to spiral out along field lines with little or no drift. If this transit time is indeed short compared to charge exchange times, one may save the divertor channel from destruction. I believe the Princeton group (Tenny and Gralnick) makes some use out of just this idea proposed by Dr. Moir in their conceptual Tokamak power reactor design.

All in all there was a great deal discussed in the meeting and a few conclusions were drawn by the attendees at the end. Listed below are some of these conslusions and recommendations:

1) There is need to do experimental work on divertors, some of which may be done by re-utilizing some already existing equipment.

2) The surface physicists should become more involved in helping the plasma physicists in the planning of their next generation experiments.

3) Consideration should be given to the idea of using a replaceable inner liner in Tokamaks thus relieving the structural wall from plasma and photon bombardment.

4) Data on sputtering properties and other surface physics phenomena should be passed on to the plasma physicists from the surface physicists ASAP.

5) Particle fluxes and energy spectra should be sent to the surface physicists from the plasma physicists ASAP.
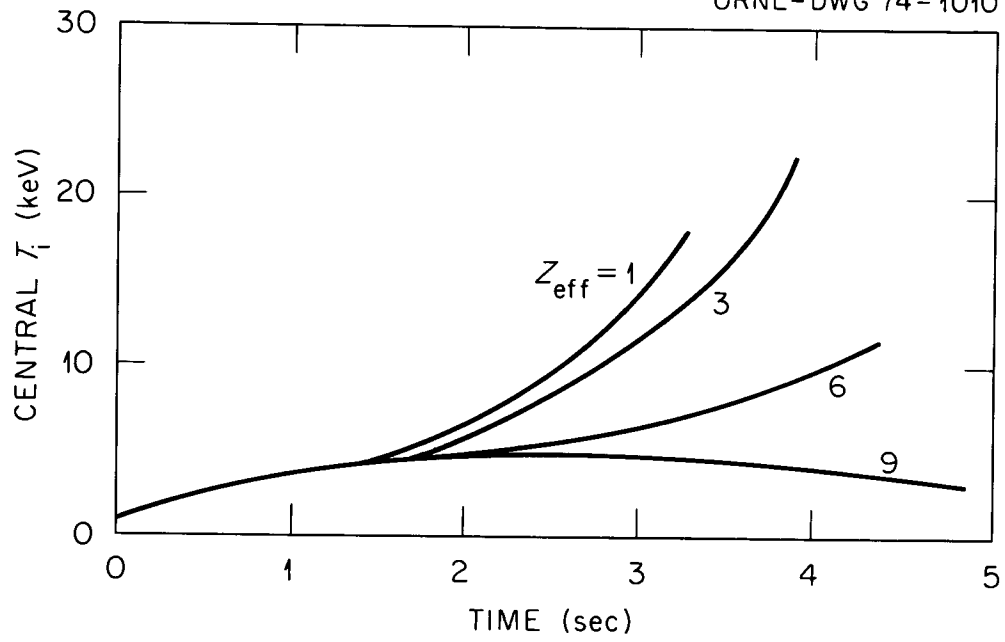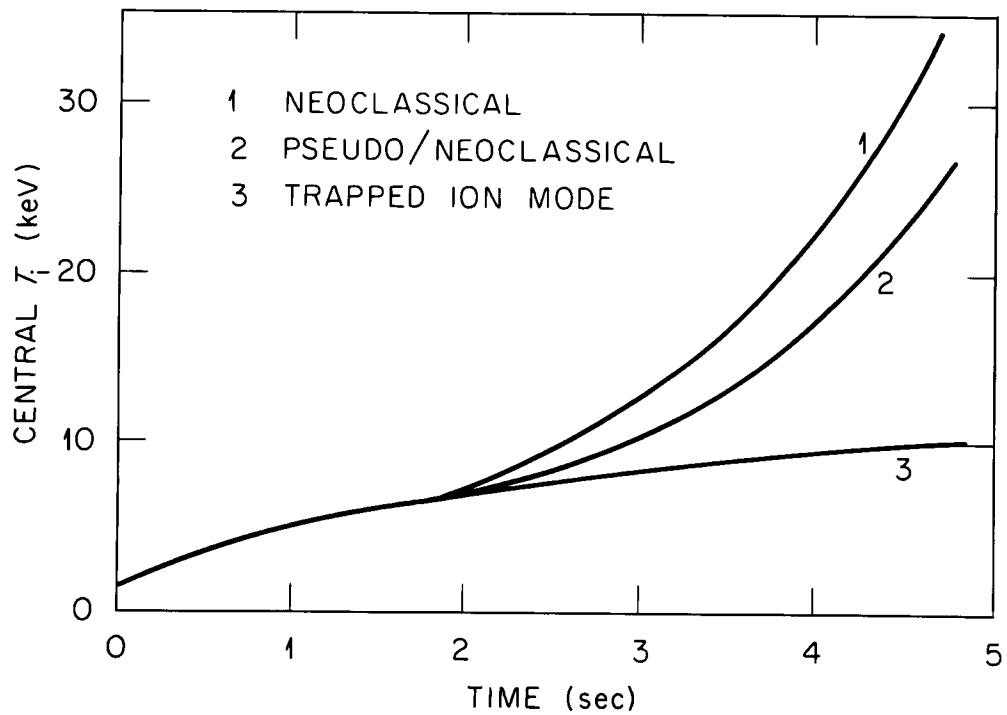
Appendix A

The following are graphs representing computer calculations by
John Hogan (ORNL). They are fairly self explanatory. It should be
noted that the ordinate lbel on the first graph is Γ_{ex}/N_{FC}. Much
of this data is discussed on ORNL-TM-4474 entitled "Fluxes of Charged
and Neutral Particles from Tokamaks", by Hogan and Clarke.
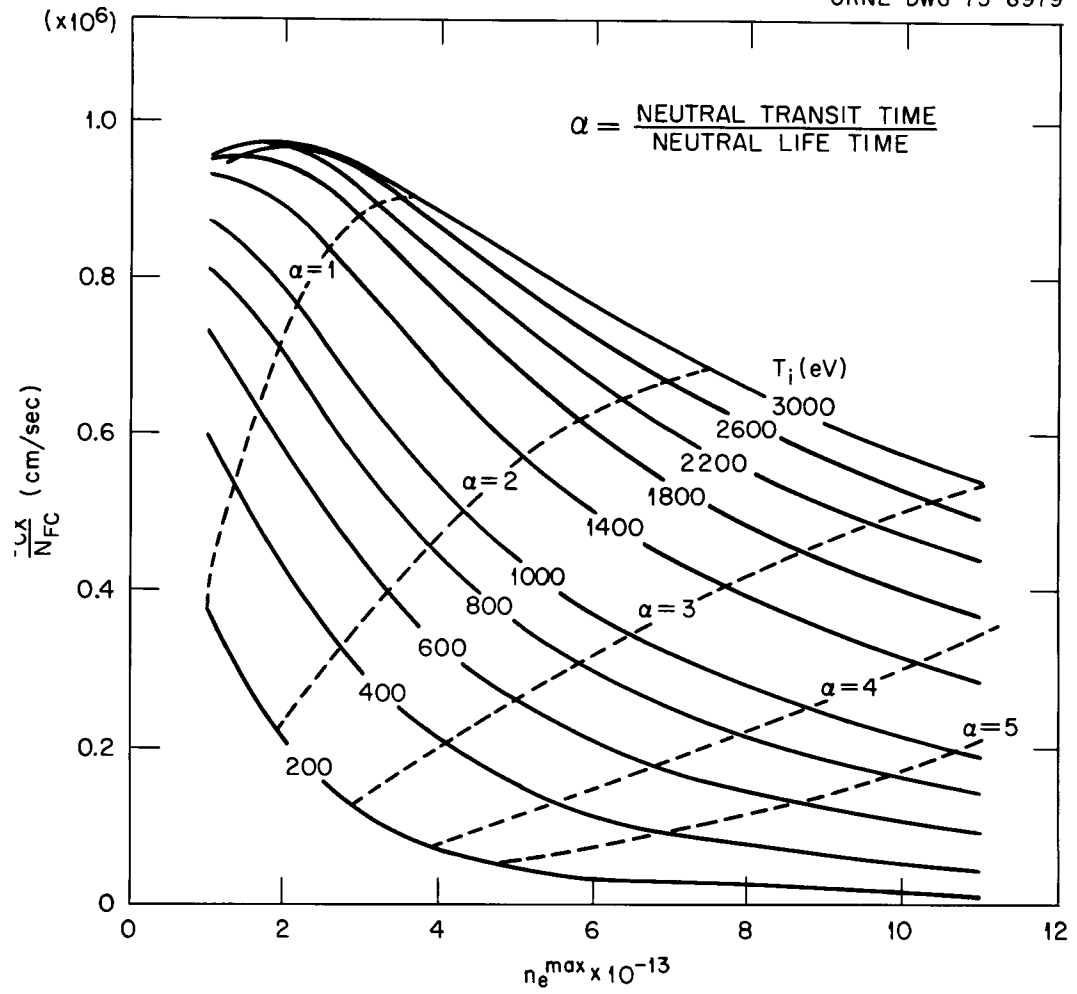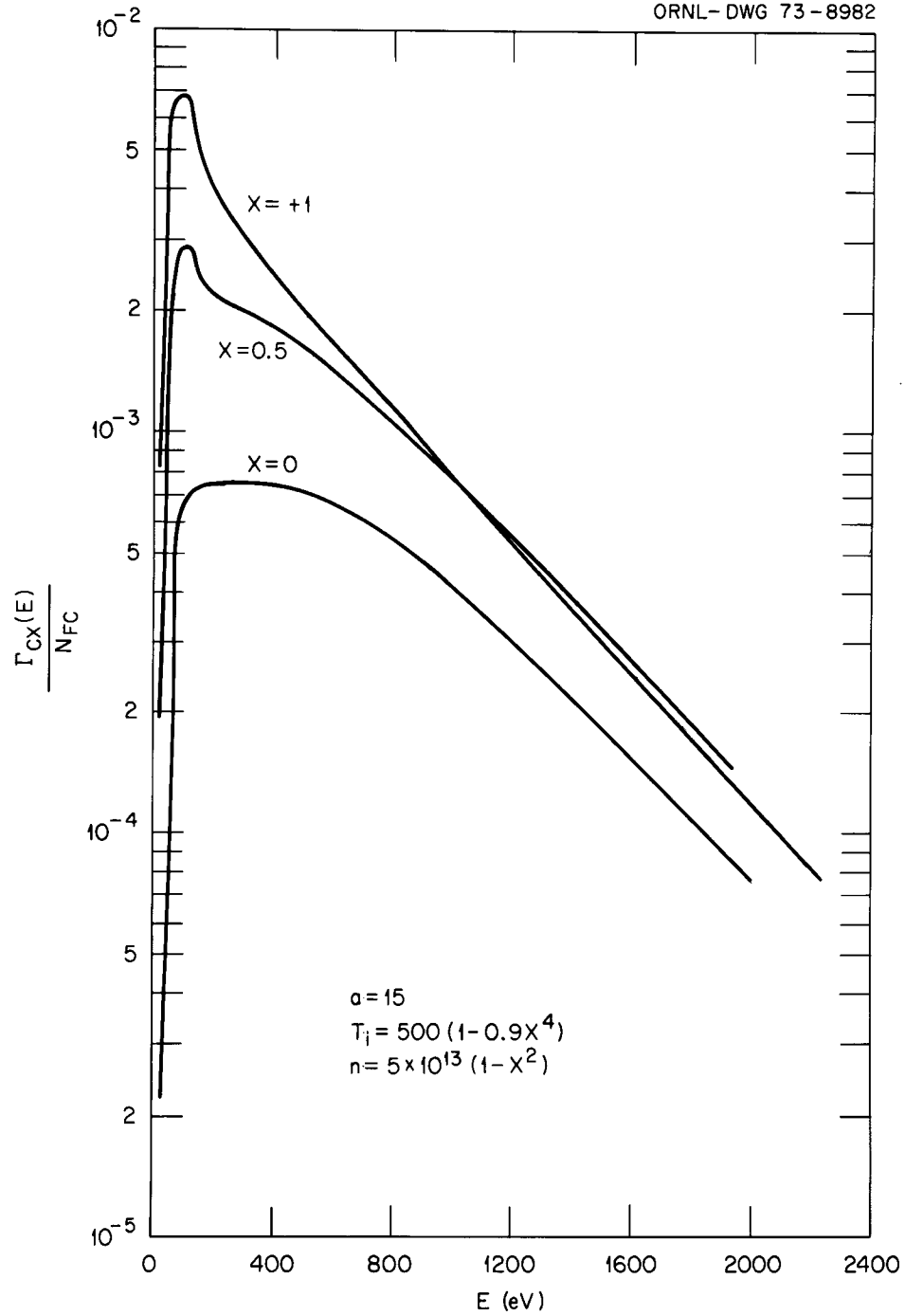
ORMAK/HFO: Charge Exchange Flux.
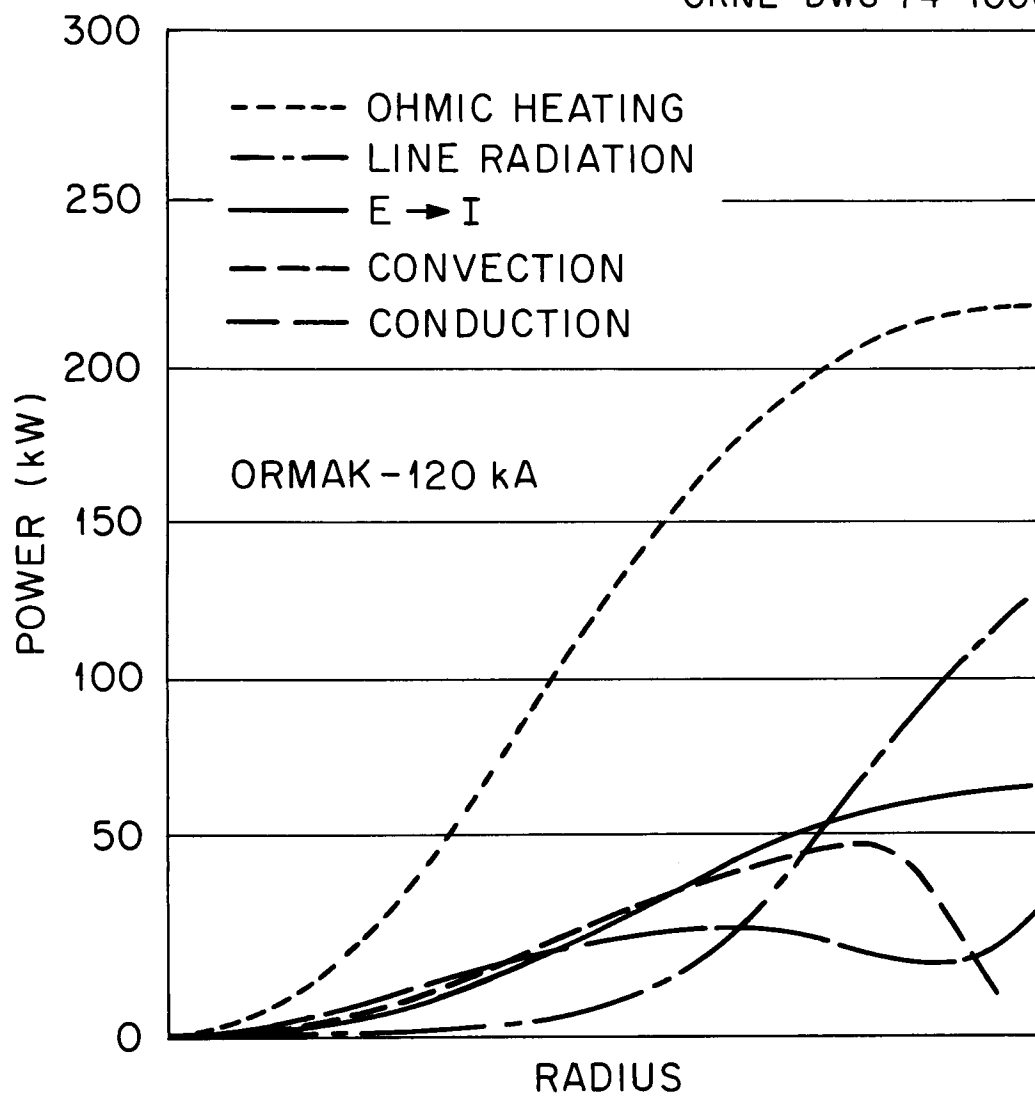
ORNL-DWG 74-1010

EFFECT OF Z_{eff} ON IGNITION

TRANSPORT MODELS

ORNL-DWG 73-8982

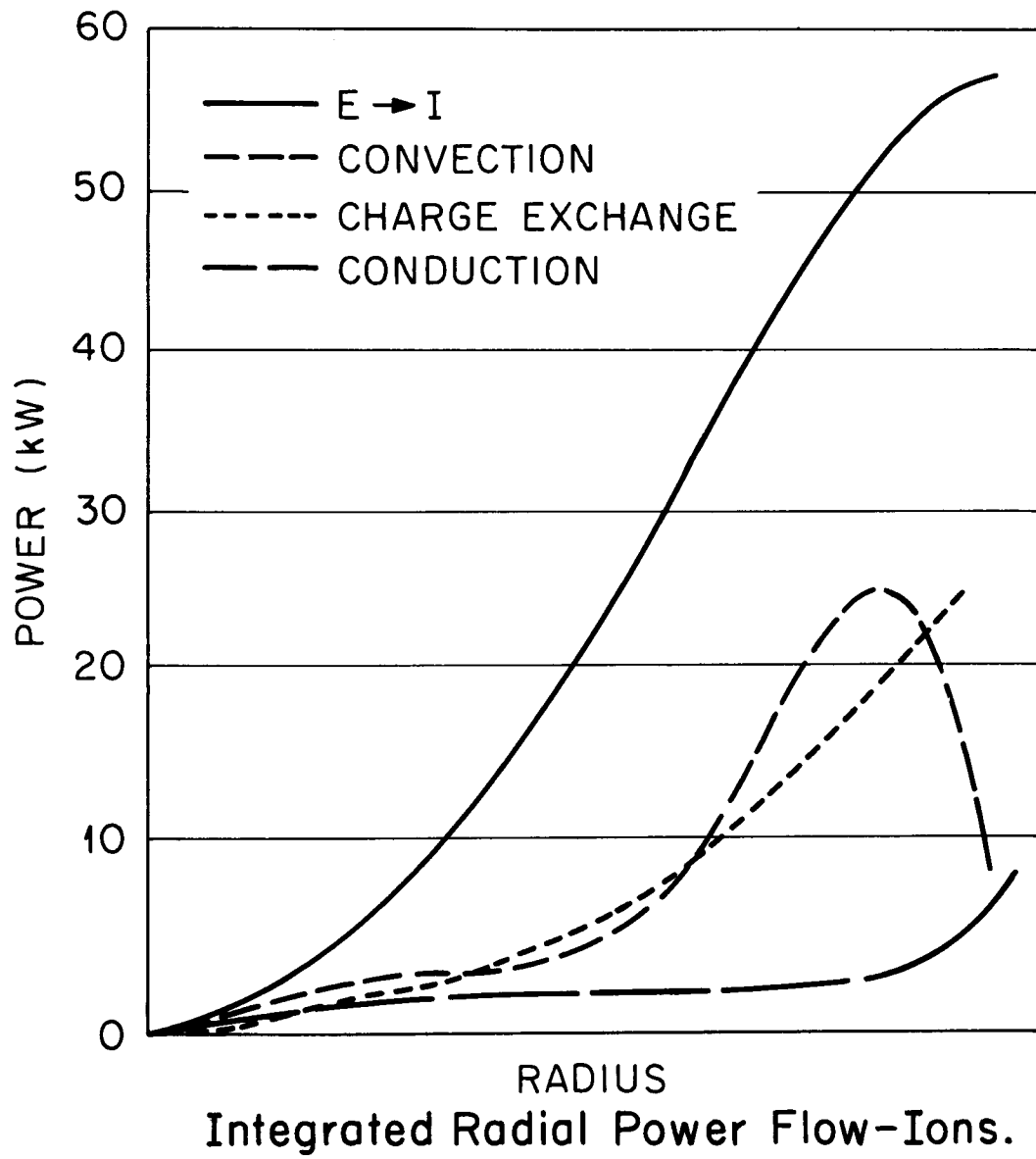Charge Exchange Neutral Spectrum vs X = r/a .

ORNL−DWG 74−1006

Integrated Radial Power Flow-Electrons.

ORNL-DWG 74-1007

Integrated Radial Power Flow-Ions.

Appendix B

The following is a copy of a paper presented by Dr. Dieter M. Gruen at the meeting on "surface Effects in Controlled Thermonuclear Fusion Devices and Reactors" which was a joint AEC-Argonne Nat'l Lab. sponsored event in Jan. 1974. The quantitative information presented at the Philadelphia meeting can be found on page B6

CHEMICAL EFFECTS OF THERMONUCLEAR PLASMA INTERACTIONS WITH INSULATOR AND METAL SURFACES*

Dieter M. Gruen
Argonne National Laboratory, Argonne, Illinois

Abstract

Deuterium and tritium, as well as plasma impurities such as oxygen and nitrogen ions, are chemically reactive particles in contradistinction to helium ions.

The interactions of chemically reactive ions with insulator and metal surfaces result in specific chemical effects which must be considered in sputtering, blistering, trapping and re-emission processes involving these projectiles. Chemical sputtering and chemical trapping of ion beam flux are examples of chemical interaction effects which are discussed.

Bombardment of a niobium surface by oxygen and nitrogen ions results in the formation of sputtered niobium oxide and nitride molecules. The molecular species are identified and characterized by means of their vibrational spectra using isotopic substitution and matrix isolation techniques. Results using matrix isolation spectroscopy for both physical and chemical sputtering studies on materials of CTR interest are presented.

Chemical trapping is evaluated as a method of chemically pumping the major fraction of the ion beam flux in the divertor of next generation Tokamaks. Suitable trapping surfaces, surface lifetimes, and reprocessing schemes are discussed on the basis of available information on trapping efficiencies and thermochemical data for a variety of metals.

Introduction

In contradistinction to noble gas ions, D^+ and T^+ are reactive particles whose interactions with insulator surfaces such as metal oxides or nitrides result in chemical reactions leading to a variety of sputtered products as well as surface compounds. The effects of such interactions can have serious consequences for the performance of insulators. For example, reduction of surface and subsurface layers to lower oxides and possibly to metal can, in principle, degrade insulating properties below acceptable levels.

Because of the paucity of quantitative work in this area, the seriousness of these effects for the performance of insulators in CTR applications remains to be assessed.

Sputtered molecules or molecular fragments which are ejected from a surface as the result of high energy collisions often involve novel or poorly characterized chemical species. Furthermore, such species have only a transitory existence under ordinary, ambient conditions of temperature and pressure. A major technique that has been employed up to now to study the nature of sputtered products has been mass-spectroscopy. A variety of important characteristics of molecules and molecular fragments, however, are not amenable to study by means of this dynamic technique. For this reason, matrix isolation spectroscopy has been developed by us as a sensitive new method to study the chemical sputtering process (1, 2).

Although there is a wealth of information about reactions of hydrogen with a wide variety of metals, the data relate almost exclusively to conditions at thermodynamic equilibrium (3). In a fusion reactor where the average particle energies are of the order of 10 Kev, pulsed modes of operation are contemplated and temperature gradients of 10^{6}°K/meter can occur, data obtained at thermodynamic equilibrium can at most be expected to furnish guidelines for the many "chemical" parameters such as the nature of compounds formed, the kinetics of reactions, the rates of diffusion, the heats of adsorption and desorption, which are characteristic of an operating fusion reactor.

The processing of large volume of D^{+} and T^{+}, after removal from the reactor, at thermal energies, and the chemical consequences of energetic particle interactions with reactor components such as the first wall, are of prime importance insofar as tritium holdup and release through permeation are concerned. The concentration of tritium in the plasma will depend in part on the rate of permeation through the first wall, and this rate may change in both magnitude and direction during the transient conditions associated with bringing the plasma to the desired steady state (or periodically pulsed) operating conditions.

A particular area of work included in the scope of the present discussion is ion beam flux trapping or "chemical pumping" at metal surfaces. The aim of work in this area is directed at achieving a better understanding of the trapping process to aid in defining a set of conditions for markedly increasing the total trapped ion beam flux per cm^{2} of metal surface (4).

circularly surround the target and direct the matrix gas toward the salt plate during matrix deposition. The target holder is electrically insulated from the rest of the system by means of a threaded, hollow nylon rod between a block at the base of the stainless tube and the brass holder. A thin insulated wire passes from the target holder to a current measuring circuit through a vacuum feedthrough at the top of the dewar. Thus, the positive ion current arriving at the target during bombardment can be measured. The independently grounded beam-defining aperture, "g", is placed in front of the salt plate assembly to limit the diameter of the incoming ion beam (indicated by the hatched arrow) to the 0.25 inch hole in the salt plate.

The back-sputtered metal atoms mix with an excess of noble-gas matrix atoms in a ratio of $\sim 1:10^3$ and codeposit on the salt plate at $\sim 14°K$. At the conclusion of the bombardment the target assembly is rotated to a position outside the radiation shield. Then the entire flange-mounted refrigerator-sample assembly is rotated 90° to allow spectroscopic measurements to be made through the dewar windows.

The absorption spectra of Au atoms in Ar, Kr and Xe matrices are shown in Fig. 2. The spectra of Ti (6), Nb (2), and Mo (7) atoms in Ar matrices are shown in Fig. 3. Each atomic species displays a characteristic matrix spectrum which can be correlated with the spectrum of the free gaseous atom.

Sputtering yields are calculated using the equation

$$S = \frac{1.158 \times 10^{-4} \times A_\sigma \times a_s}{f_{\ell u}^{(m)} \times G \times C \times I \times t}$$

where

A_σ = integrated absorbance over an absorption band

a_s = the area of the salt plate sampled by the spectrometer beam

$f_{\ell u}^{(m)}$ = oscillator strength (in the matrix) of the atomic transition

G = geometric factor, calculated assuming a cosine distribution of sputtered products

C = sticking coefficient

$I \times t$ = integrated ion beam current to the target

Results already obtained on sputtering yield determinations of Au and Nb indicate that continued development of the matrix technique will provide a rapid and sensitive new method for measurements of this kind.

B. Chemical Sputtering

Bombardment of a Nb metal target with oxygen and nitrogen ions results in addition to sputtered Nb metal atoms, in the ejection of NbO and NbN molecules respectively. The molecular sputtered products were identified by means of their infrared spectra using isotopic substitution techniques. Table I reports the observed frequencies for $Nb^{16}O$ and $Nb^{18}O$ and the observed and calculated ρ values:

$$\rho_{obs} = \nu(Nb^{18}O)/\nu(Nb^{16}O), \quad \rho_{calc} = [\mu(Nb^{16}O)/\mu(Nb^{18}O)]^{1/2} .$$

ν is the observed frequency and μ is the reduced mass (8).

The uncertainty in frequency measurements (less than 1.0 cm^{-1}) leads to an uncertainty of less than 0.0010 in ρ_{obs}; the anharmonic correction to an uncertainty of less than 0.0004. The agreement of ρ_{obs} and ρ_{calc} in Table I confirms the assignment to NbO. Furthermore, no additional features were observed in a mixed $^{18}O_2/^{16}O_2$ experiment eliminating the possibility that the absorber contains more than one equivalent O atom. Agreement with the observed gas phase $\Delta G_{1/2}(981.3_7$ cm$^{-1})$ of the $^4\Sigma^-$ state is good taking account of the expected matrix shift. The origin of the observed triplet structure for $Nb^{16}O$ and $Nb^{18}O$ is likely multiple stable matrix sites.

TABLE I
Observed Frequencies of $Nb^{16}O$ and $Nb^{18}O$ Isolated in
an Ar Matrix at 14°K with Observed and Calculated ρ Values

$Nb^{16}O$ obs $\Delta G_{1/2}$ (cm^{-1})	$Nb^{18}O$ obs $\Delta G_{1/2}$ (cm^{-1})	ρ obs	ρ calc
964	918	0.952_3	0.9513
968	921	0.951_4	0.9513
971	924	0.951_6	0.9513

TABLE II
Observed Frequencies of $Nb^{14}N$ and $Nb^{15}N$ Isolated in
an Ar Matrix at 14°K with Observed and Calculated ρ Values

$Nb^{14}N$ obs $\Delta G_{1/2}$ (cm^{-1})	$Nb^{15}N$ obs $\Delta G_{1/2}$ (cm^{-1})	ρ obs	ρ calc
1002.5	974	0.971_6	0.9707

Partial analysis of the visible spectra of $Nb^{16}O$ and $Nb^{18}O$ has shown a ν' progression (0-0 through 3-0) of an electronic transition with average $\Delta G'_{1/2}(Nb^{16}O)$ = 894 and $\Delta G'_{1/2}(Nb^{18}O)$ = 894 cm^{-1}. The value of ρ_{obs} = 0.949$_7$ is in satisfactory agreement with ρ_{calc} = 0.9513. The band origin for $Nb^{16}O$ is about 15 364 cm^{-1} (650.7 nm). The band origin and vibrational spacing are in agreement with gas phase values for the $^4\Pi$-$^4\Sigma^-$ transition. Additional bands in this spectral region have not been fully analyzed, but the present data support the assignment of a $^4\Sigma^-$ electronic ground state for NbO.

Table II reports the results for $Nb^{14}N$ and $Nb^{15}N$. The agreement of calculated and observed ρ values is within experimental uncertainties. No additional features were observed in a mixed $^{14}N_2/^{15}N_2$ experiment.

Study of the other observed ir absorption of $Nb-O_2$ species as well as the visible spectrum of both NbO and NbN is in progress.

The Mechanism of Chemical Trapping of Deuterium in Metals

Among the chemical effects of energetic plasma particle interactions with metals, the trapping of D^+ and T^+ by certain metals can potentially be an extremely useful phenomenon for pumping and processing the thermo-nuclear fuel.

To gain an appreciation of the magnitude of the problems associated with plasma processing in a full-scale fusion reactor, a consideration of the relevant design parameters is in order. For the purposes of this discussion, consider a toroidal D-T reactor with total thermal fusion power of 5500 MW achieved by the fusion of 0.0023 moles of DT/second (9). The daily fuel consumption in the plasma is 0.39 kg D and 0.575 kg T while the production of He^4 is 0.77 kg. For reasonable fuel burnup (3.9%), it turns out that close to 0.1 mole or $\sim$6 x 10^{22} plasma particles (D^+, T^+, He^+) must be removed from the reactor every second. An equal number of D and T particles must, of course, be reinjected into the reactor every second to provide new fuel. To handle this amount of gas at thermal energies in conventional vacuum systems requires a throughput of $\sim$3000 torr liter/sec. In turn, to maintain a base pressure of 10^{-5} torr, a pumping speed of 10^9 liters/sec is required. These numbers indicate the magnitude of the vacuum pumping problem for a gas at thermal energies. However, the particles arrive in the divertor region with their full plasma kinetic energy. They must therefore be slowed down and thermalized before they can be handled in conventional systems of whatever size as thermal gas.

If the incoming D^+ and T^+ ions could be immediately trapped when first striking a surface in the divertor, pumping speed requirements would be reduced by a factor of 20 assuming 5% burnup and zero trapping of He^+.

Studies of deuterium trapping in solid targets have shown its dependence both on bombardment time and target temperature (10).

These results can be understood on the basis of the following considerations. After slowing to thermal energies, the ions diffuse through the solid lattice but on reaching the surface encounter a potential barrier inhibiting their escape due to the heat of solution of deuterium in the metal. The escape probability is given by $e^{-Q/RT}$ where Q is the heat of solution. The "trapped" deuterium will be able to diffuse through the lattice without being able to escape from the surface over a certain temperature range because the activation energies for diffusion are much lower, $\sim$5 kcal/mole, than the heats of solution, 20-60 kcal/mole. The decreasing trapping efficiencies at higher temperatures are due to the increasing probability of the diffusing D atoms to overcome the potential barrier for escape from the surface. Furthermore, it appears that as the surface layers are converted to a bulk deuteride (or tritide) phase, no further uptake of deuterium occurs. The elucidation of this rejection phenomenon is of fundamental importance to an understanding of the trapping mechanism and therefore to the ultimate practical utilization of trapping as a means of handling thermonuclear plasmas. The chemical sputtering studies described above are being extended to shed light on various aspects of the chemical trapping mechanism.

Although materials development and a more detailed knowledge of the trapping process will undoubtedly allow one to trap larger numbers of D and T particles per cm^2 than current experiments would indicate, we will use the number 10^{21} particles/cm^2 to calculate the exposure time of a trapping surface (11). With 6×10^{22} particles leaving the reactor per second and a trapping surface area of 5×10^5 cm^2, the surface would have to be renewed every 8300 seconds. If the surface were that of a continuously moving strip of Ti metal 20 cm in width and 2.5×10^4 cm long, its velocity would have to be 3 cm/sec. One mole of TiD_2 (TiT_2) would be produced every 10 seconds leading to a total production rate of 200 kg per day. If the total thickness of the Ti strip is 1 mm, a layer 0.1 mm thick will be converted to TiD_2 (TiT_2). About two tons of Ti would have to be processed each day to recover the D and T.

The above discussion illustrates that the unprecedented fluences of energetic D^+, T^+ and He^+ to which trapping surfaces are exposed in the divertor region of a toroidal fusion reactor present a series of problems each of which must be studied in detail before a realistic appraisal of the feasibility of this technique for plasma handling can be fully evaluated.

References

*Work performed under the auspices of the U. S. Atomic Energy Commission.

1. D. M. Gruen, S. L. Gaudioso, R. L. McBeth and J. L. Lerner, J. Chem. Phys., In Press.

2. D. W. Green, D. M. Gruen, F. Schreiner and J. L. Lerner, Applied Spectroscopy, In Press.

3. "Metal Hydrides", W. M. Mueller, J. P. Blackledge and G. G. Libowitz, editors, Academic Press, New York (1968).

4. D. M. Gruen in "The Chemistry of Fusion Technology", D. M. Gruen, editor, Plenum Press, New York (1972).

5. A. J. Summers, N. J. Freeman and N. R. Daly, Paper 4.1, B.N.E.S. Nuclear Fusion Reactor Conf., Culham, England (1969).

6. D. M. Gruen and D. H. W. Carstens, J. Chem. Phys. 54, 5206 (1971).

7. D. W. Green and D. M. Gruen, J. Chem. Phys., In Press.

8. D. W. Green, W. Korfmacher and D. M. Gruen, J. Chem. Phys. 58, 404 (1973).

9. E. F. Johnson in "The Chemistry of Fusion Technology", D. M. Gruen, editor, Plenum Press, New York (1972).

10. G. M. McCracken and S. K. Erents, Paper 4.2, B.N.E.S. Nuclear Fusion Reactor Conf., Culham, England (1969).

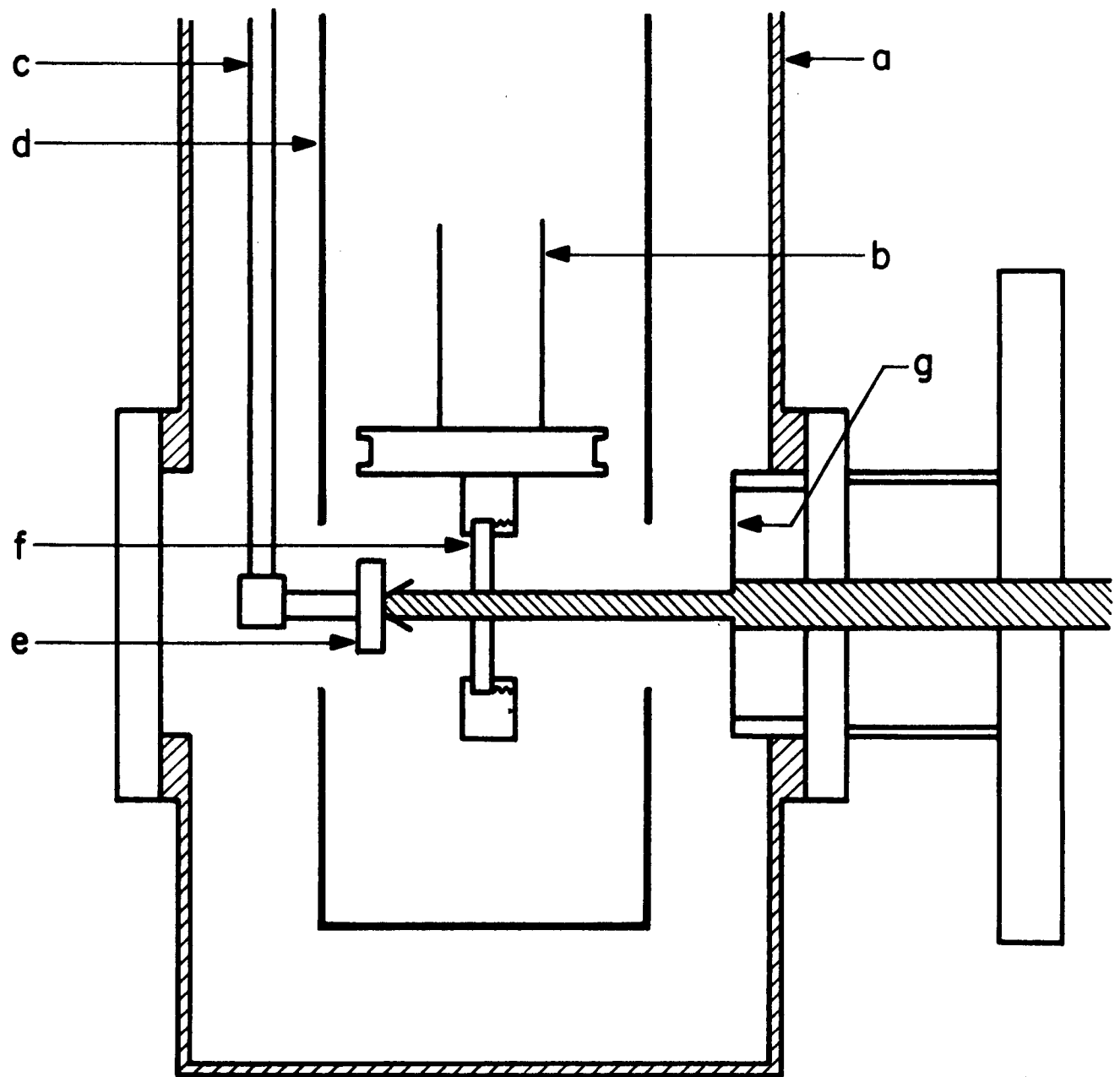11. O. C. Yonts and R. A. Strehlow, J. Appl. Phys. 33, 2903 (1962).

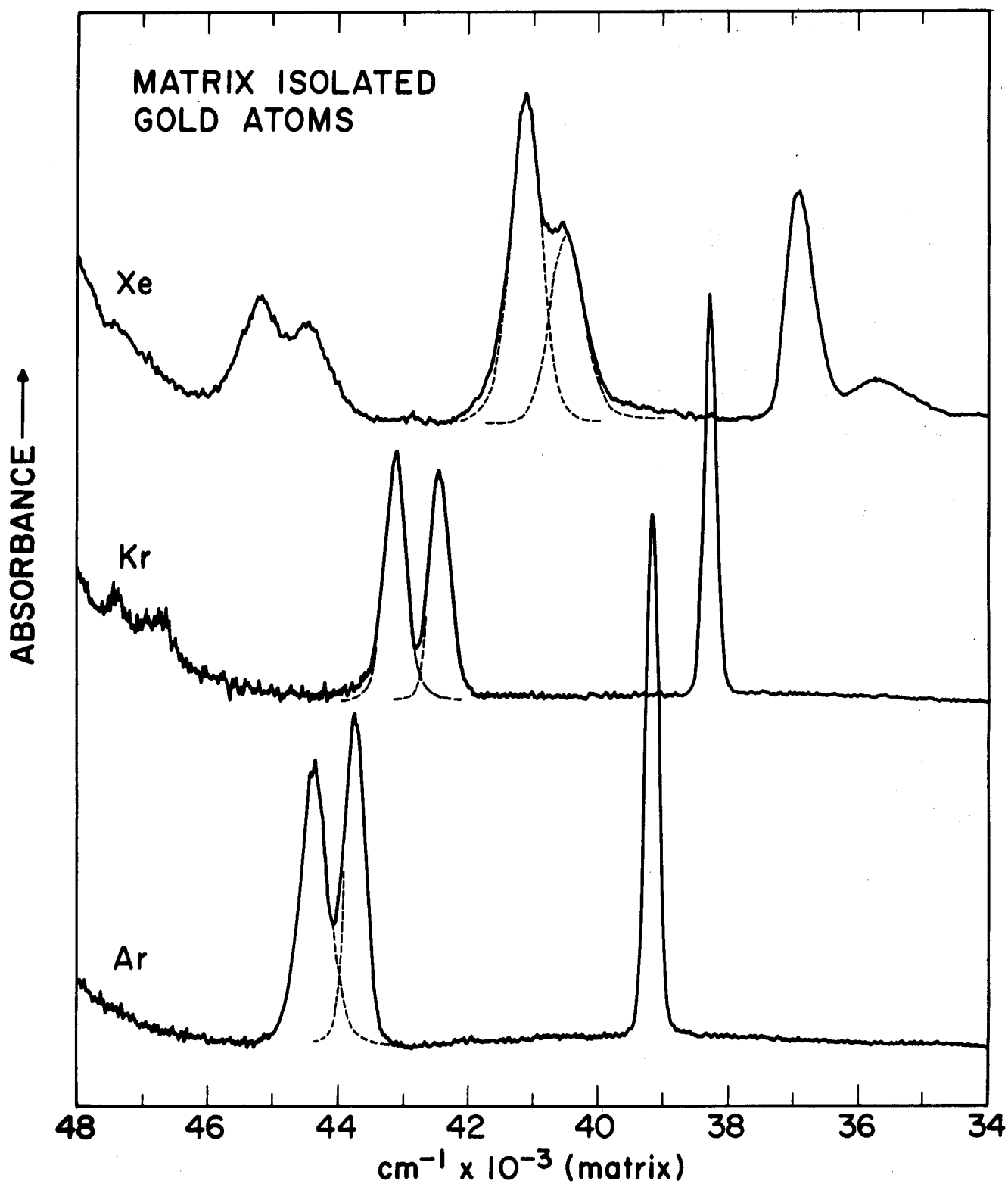Fig. 1. Sputtering target-matrix isolation assembly

Fig. 2. Resonance transitions of Au atoms isolated in Ar, Kr and Xe matrices at 14°K.
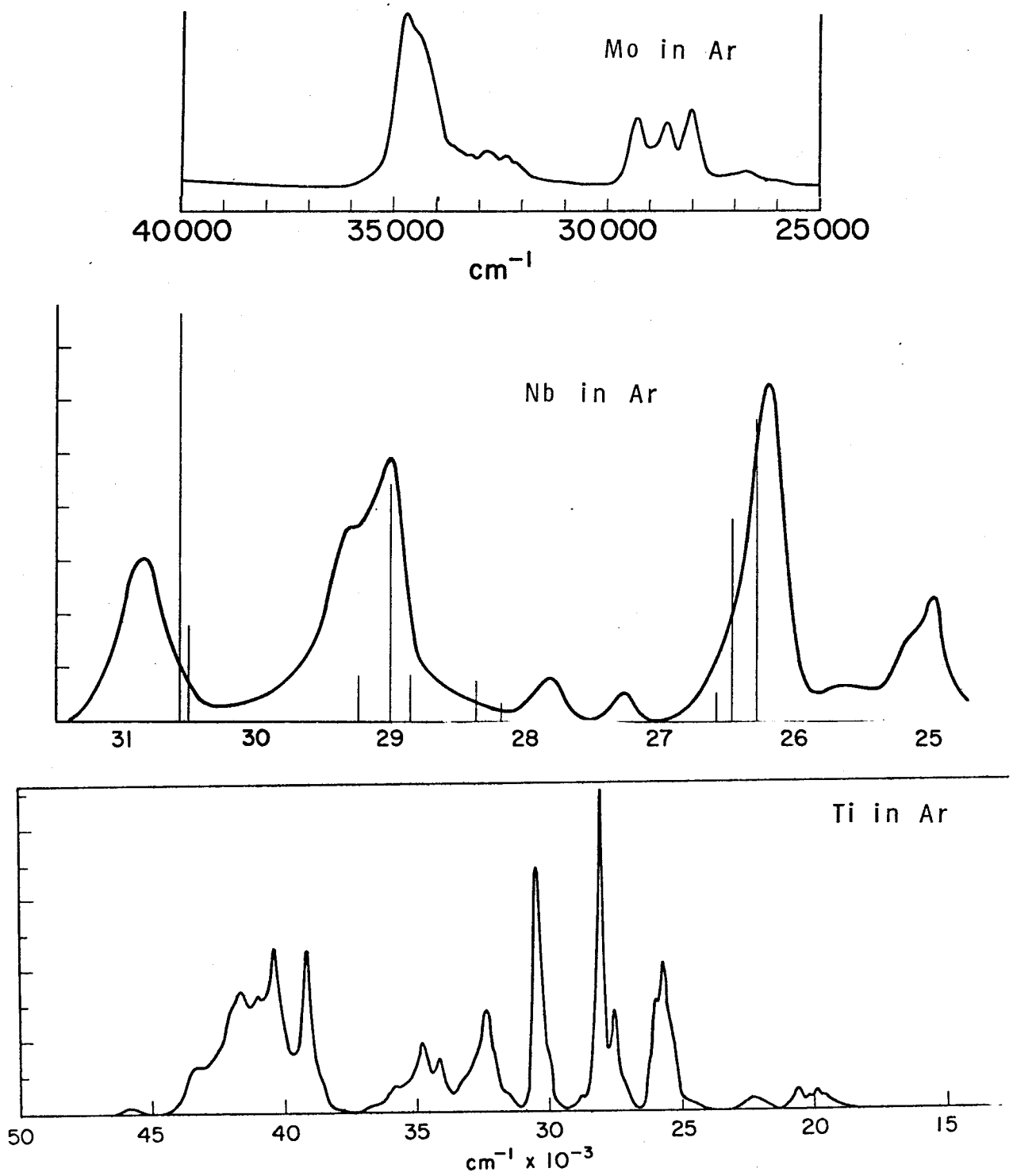
Fig. 3. Absorption spectra of Mo atoms (top), Nb atoms (middle), Ti atoms (bottom) in Ar matrices at 14°K.

Appendix C

Presented here is a short report from Dr. Ben Feinberg who performed his Ph.D. research at Columbia on this topic. Dr. Feinberg has kindly provided a copy of this article (submitted for publication in   , which covers essentially all of Dr. Gross's talk.

The Application of Matrix Isolation Spectroscopy to Quantitative Sputtering Studies

A. Sputtered Metal Atoms

Matrix isolation is a technique for capturing and immobilizing transient or reactive species in an inert, usually a noble gas matrix by codeposition on a cold surface. After deposition, the reactive species are prevented from reacting with each other by bimolecular collisions because the matrix temperature is too low to allow diffusion to occur. Furthermore, the energy remaining to the reactive species is too small to lead to unimolecular decomposition. As a result, sufficient numbers of sputtered atoms or molecules can be collected in a matrix to provide a sample large enough for spectroscopic examination.

Because the matrix isolation method for measuring sputtering yields does not require a weight loss determination of the target material, it is of particular interest for establishing D^+ and T^+ sputtering yields of metals such as Nb, V, Ti and Zr which tend to absorb and retain the bombarding projectiles, thus in fact experiencing a weight gain during bombardment (5). The sensitivity of the method for the detection of metal atoms has already been developed to the extent that a quantity of sputtered atoms equivalent to 0.1 monolayer can be determined with good accuracy. Improvements in sensitivity by two orders of magnitude can be expected (1).

The process of sputtering and of sputtered atom collection take place within the evacuated target-collector assembly illustrated in Fig. 1. The main dewar body is designated by "a". A closed-cycle He refrigerator is attached to a flange (not shown) at the top of the dewar. A copper sample block, indicated by "b", is mounted directly to the second stage of the refrigerator. This block has provision for mounting a one inch diameter sodium chloride plate, "f", which is cooled to 14°K during refrigerator operation. The salt plate has a 0.25 inch diameter hole through its center which geometrically defines the mass and energy selected ion beam and allows it to strike the target. A copper radiation shield, "d", is attached to the first stage of the refrigerator and surrounds the sample block. Suitable openings are provided for the entering ion beam and the target assembly. The hollow stainless steel tube, "c", serves a dual purpose. It supports the target and provides a means of conducting the matrix gas into the dewar. The hollow brass target holder, "e", has the appropriate metal foil targets mounted on its face. Six 0.0156 inch holes

A STUDY OF HOT PLASMA IN CONTACT WITH A COLD WALL

B. Feinberg and R.A. Gross
Plasma Laboratory, Columbia University, N.Y.,N.Y.

Abstract

A study has been made of the energy transfer from a hot $(T \sim 5 \times 10^6 \, {}^{\circ}K)$ plasma containing a strong magnetic field brought into sudden contact with a cold wall. The rate of energy transfer has been measured and compared with theoretical predictions. Photographs obtained with a scanning electron microscope of wall surface damage are presented.

Introduction

When a hot plasma comes into contact with a cold wall, as it does sooner or later in all plasma devices, the plasma loses its energy to the wall. The physically important problem of a plasma initially with a uniform temperature and a strong magnetic field parallel to the wall has been studied analytically for simple cases, and by computer simulation for more realistic cases, by M.S.Chu (1). For a deuterium plasma of negligible resistivity, and classical plasma thermal conductivity, the rate of heat transfer from the hot plasma to a cold wall q is,

$$q = T \left(\frac{K_\perp \rho k}{(\gamma - 1)\pi m t}\right)^{\frac{1}{2}} \approx 3.72 \times 10^{-24} \left[\frac{T^{3/2} n_i^3 \ln \Lambda}{B^2 t}\right]^{\frac{1}{2}} \text{ watts/cm}^2 \qquad (1)$$

where T is the initial uniform plasma temperature, $K_\perp$ is the transverse plasma thermal conductivity, ρ is the plasma density, k is Boltzmann's constant, γ is the ratio of specific heats, m is the ion mass, t is the time, n_i is the ion number density, $\ln \Lambda$ is the usual plasma Coulomb logarithm, and B is the magnetic field strength. The variables in equation (1) are in cgs units. The effects of variable resistivity, thermal conductivity, convection, and nonequilibria have been studied by Chu who numerically solved the relevant equations. For this purpose he used multifluid plasma equations, and although there are detailed differences from the analytical solution of equation (1), the biggest physical uncertainty is whether the plasma thermal conductivity can be represented by its classical (laminar) value. Many situations in plasma physics have been found where the classical transport properties do not properly nor accurately describe the situation. Consequently a series of experiments were

so that an exact comparison is no longer valid. The somewhat larger
energy transfer rate that is observed may be explained in part by heating
from convection and thermoelectric effects, which are not included in the
classical equation. Whether the surface of the material melts can be
estimated (1) by noting the nature of the thermal conductivity of the
material and the energy flux at the surface, which scales like $t^{-\frac{1}{2}}$. The
greatest damage should occur at the very earliest times, when the energy
flux to the wall is greatest, and the fluid equations are not valid. The
ion gyro period is of the order of 10^{-7} sec for the case studied, and dur-
ing that time about 10^{15} particles/cm^2 (those particles which are within a
gyroradius of the wall) strike the surface. If they are 1 keV particles,
the power flux to the wall is about 5×10^{6} watts/cm^2 during this first gyro
time period. It is this plasma near the surface which will do most of the
early damage to the wall since later the plasma cools and forms a protec-
tive gas blanket next to the wall.

Three material samples were examined using the scanning electron mic-
roscope and they are shown in subsequent figures. It is rather clear that
in the stainless steel and boron nitride cases, the surface material has
melted and been eroded. The depth of the valleys in the stainless steel is
of the order of five microns. The copper surface shows some aluminum nod-
ules which were melted elsewhere in the shock tube and redeposited on the
copper surface. The copper surface itself shows very little effects of
melting.

References

1. M.S. Chu, Phys. Flds 16, 1441 (1973).

2. B. Feinberg, Ph.D. thesis, Columbia University, New York (1973).

3. R.A. Gross, Y.G. Chen, E. Halmoy, P. Moriette, Phys. Rev. Letters 25,
    575 (1970); also: Y.G. Chen, C.K. Chu, R.A. Gross, E. Halmoy, P. Moriette
    and S. Schneider, Proc. 4th IAEA Conf., Madison, Wisconsin, June 1971,
    Vol.III, pp.241; also, E. Halmoy, Phys. Flds 14, 2134 (1971); also P.
    Moriette, Phys. Flds 15, 51 (1972).

performed by Feinberg (2) to test the validity of the classical plasma heat transfer equation.
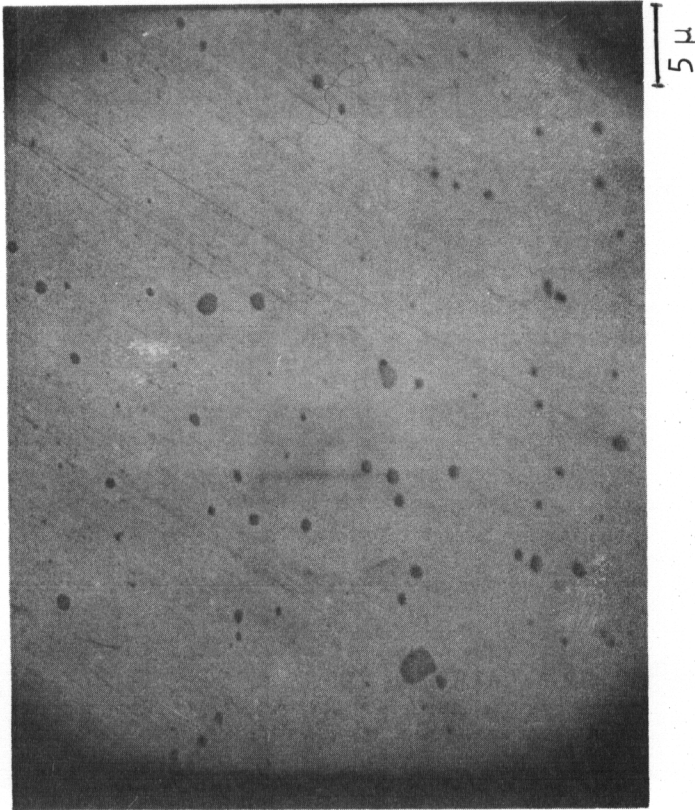
The Experiment

The Columbia high energy electromagnetic shock tube can produce several liters of hot (T ~ 5 x 10^6 $^\circ$K), dense (n ~ 10^{16} cm^{-3}) plasma. This device has been described by several authors (3). The plasma contains a strong magnetic field (B ~ 10^4 G) parallel to the walls of the device, and upon shock reflection from an end wall, the physical situation described in the introduction is very well emulated. Feinberg developed a fast response (~ 200 nanosec), thin film, heat transfer gauge. It consists of a thin film (~ 2000 Å) of carbon deposited on a sapphire window. The carbon layer is covered by a 1500 Å thick layer of aluminum to make the gauge opaque to infrared radiation from the hot plasma. The sapphire window is mounted with its thin film flush with the interior wall of the shock tube. When the hot plasma is brought into sudden contact with the wall (and the gauge), the carbon film temperature rises to several hundred degrees Kelvin. The warm carbon radiates in the infrared, and this radiation is collected by an external optical system which focuses the radiation on a Ge:Au detector. This system has been calibrated in situo using a black body source. By thus measuring the temperature of the carbon film as a function of time, the energy transfer rate from the hot plasma to the cold wall was experimentally determined. Details of the heat transfer gauge and the experimental technique can be found in reference 2.

In addition to the series of heat transfer measurements, observations have been made on the nature and amount of damage sustained by several different materials when the plasma is brought into sudden contact with them. The solid materials were polished using standard metallurical techniques. They were then mounted with the polished surface flush with the interior of the shock tube wall. These wall samples remained in this location for several hundred shots of the shock tube, after which they were removed and examined using a scanning electron microscope.

Results

A sample of the heat transfer data is shown in the first figure. At early times, the energy transfer rate is seen to agree with the classical prediction, although after about the first microsecond the energy transfer rate deviates and is higher than predicted by the classical formula. After about 3 microseconds, an expansion fan begins to cool and dilute the plasma
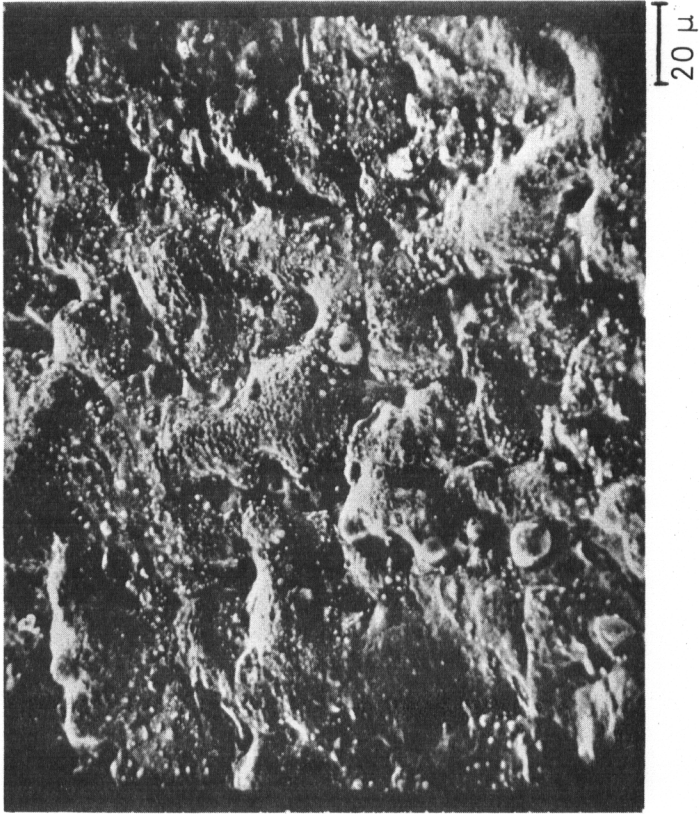
Scanning electron micrograph of a stainless steel surface.

Before exposure;

magnification 2300

After exposure to plasma
and electric currents;

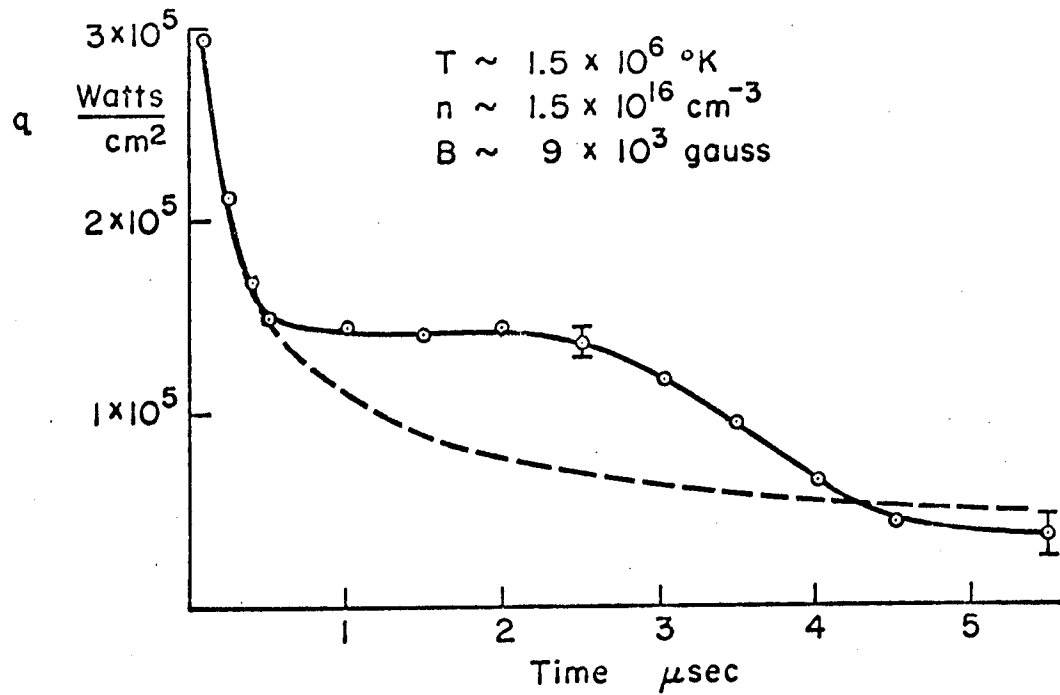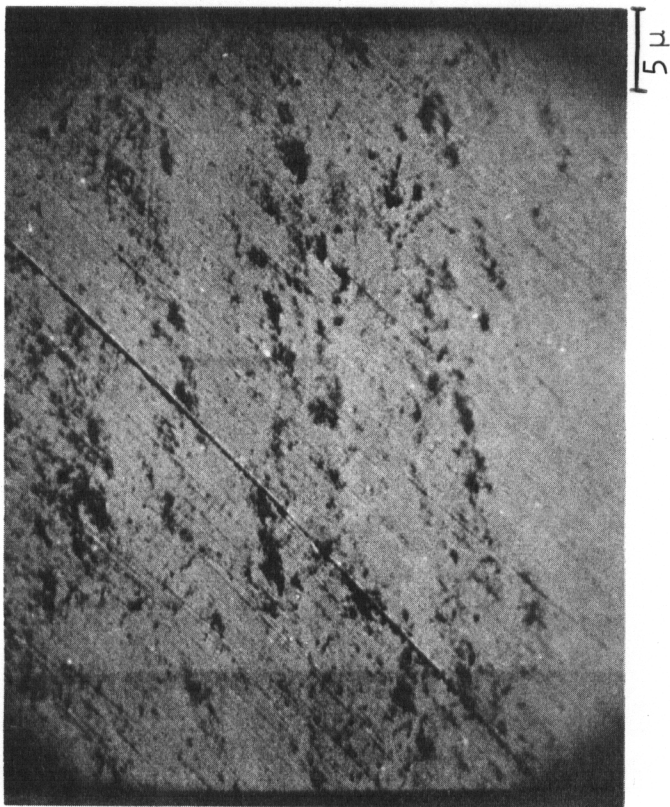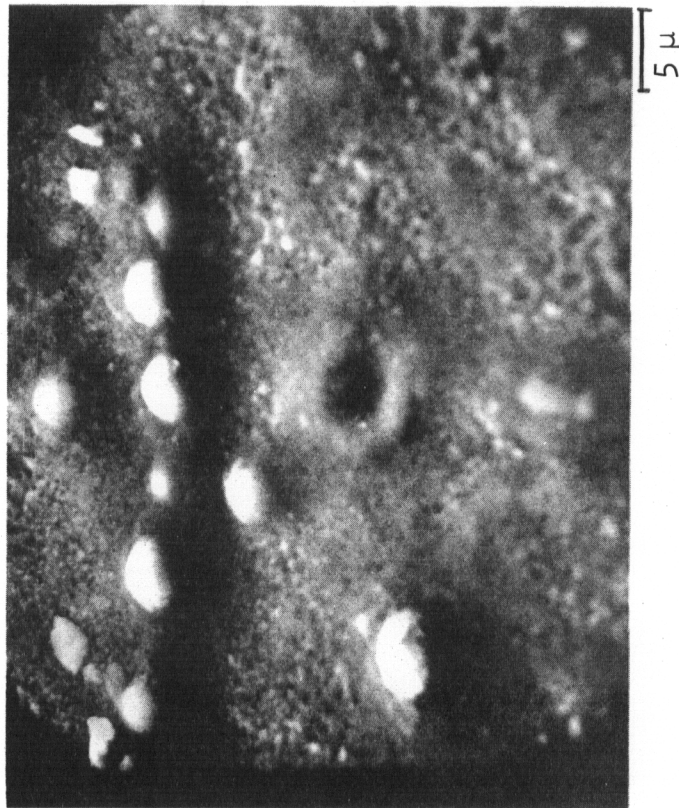magnification 530

number of shots = 625

FIGURE 2

FIG 1

The solid line is the experimentally measured heat transfer from the plasma to the wall. The dashed line is equation (1).

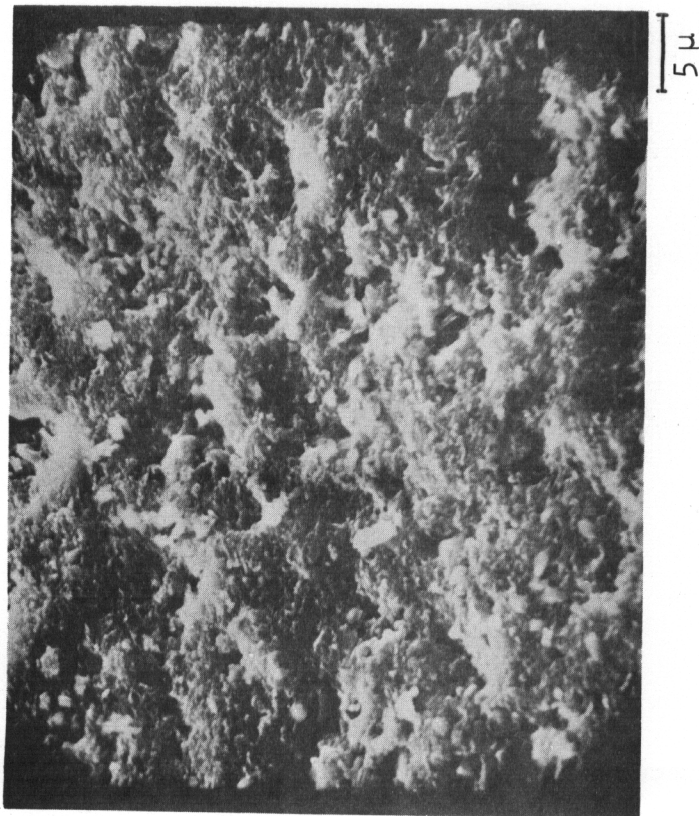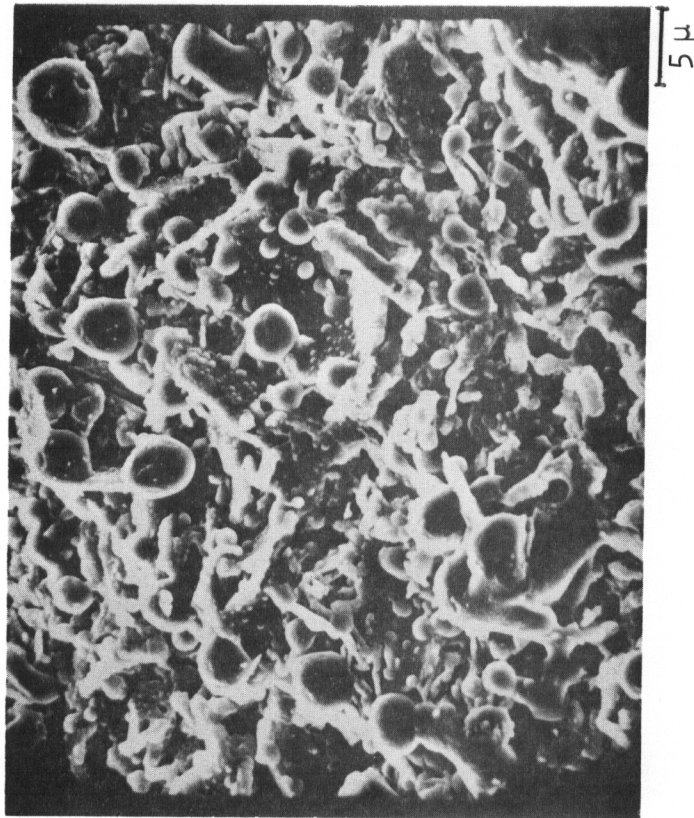Scanning electron micrograph of a copper surface.

Before exposure;
magnification 2150

After exposure to ninety plasma
shots and very high electric currents.
magnification 2250

FIGURE 3

Scanning electron micrograph of a boron nitride surface.

Before exposure;
magnification 2000

After exposure to 500 plasma
shots and very high electric currents.
magnification 2150

FIGURE 4

Appendix D

Reproduced here with permission is a copy of an article by
Walter Bauer and G. J. Thomas which appeared in the Journal of
Nuclear Materials in 1973.

LETTERS TO THE EDITORS – LETTRES AUX REDACTEURS

HELIUM RE-EMISSION AND SURFACE DEFORMATION IN 316 STAINLESS STEEL DURING –170°C TO 700°C IMPLANTATIONS *

Walter BAUER

Sandia Laboratories, Livermore, California, USA

G.J. THOMAS

Sandia Laboratories, Albuquerque, New Mexico, USA

A number of recent publications [1–4] have appeared on He re-emission and blister formation upon He bombardment of metals at a variety of temperatures. Kaminsky and Das [1] observed blister formation in mono- and poly-crystalline Nb at 900°C. They found the surface morphology to be dependent upon the state of cold-work of the samples and also observed a temperature dependence. Erents and McCracken [2] investigated the He re-emission and blister formation in Mo upon He bombardment. They found that blister formation occurred after a critical dose of $\sim 5 \times 10^{17}$ ions/cm^2 (20 keV He ions) and that the appearance of the blisters coincided with gas release from the surface. Bauer and Morse [3] investigated the He re-emission in Nb during bombardment at temperatures from $-170°C$ to $700°C$. They observed a sudden increase in the re-emission at a dose of 1 to 1.5×10^{18} helium atoms/cm^2 at elevated temperatures but a more gradual increase at lower temperatures. Thomas and Bauer [4, 5] investigated blister formation and He release spectra in Pd from $-170°C$ to $700°C$. In addition to the dose dependence, a strong temperature dependence of the blister formation and He release spectra was observed. They concluded that migration of intrinsic defects may play a role in the formation of helium defect configurations during implantation at elevated temperatures.

In this work we report He re-emission measurements in 316 stainless steel during 300 keV implantation to

4×10^{18} He atoms/cm^2 at temperatures between $-170°C$ and $700°C$. The nature of the surface deformation was optically determined on the same sample during implantation and via scanning electron microscopy after implantation. This approach allows a simultaneous comparison to be made between surface blister morphology and He re-emission. Stainless steel was chosen for this investigation because of its technological importance and the lower temperature range of its vacancy mobility ($\lesssim 500°C$) as compared to the b.c.c. metals ($\lesssim 800°C$).

The samples used in these experiments were mechanically polished to an optical finish on one side, annealed at 700°C for 1 h and cooled slowly. This pretreatment was chosen so that during the highest implantation temperature (700°C) no further substantial microstructural changes occur. Examination of the samples after annealing showed chromium-rich carbide precipitates which are preferentially located on surface scratches and grain boundaries. The precipitates, while playing a role in the nucleation of microscopic He bubbles, are believed to be of secondary importance to the blister formation mechanisms discussed in this report. The re-emission measurements were conducted on the Sandia Livermore 450 keV positive ion accelerator with the target chamber directly connected to a high-sensitivity helium mass spectrometer. The helium beam was reduced to its final size of 0.1 cm^2 by two apertures of 0.3 cm^2 and 0.1 cm^2 before entering the sample chamber. A vacuum system was attached to the chamber separating the two apertures. This served to decouple the helium
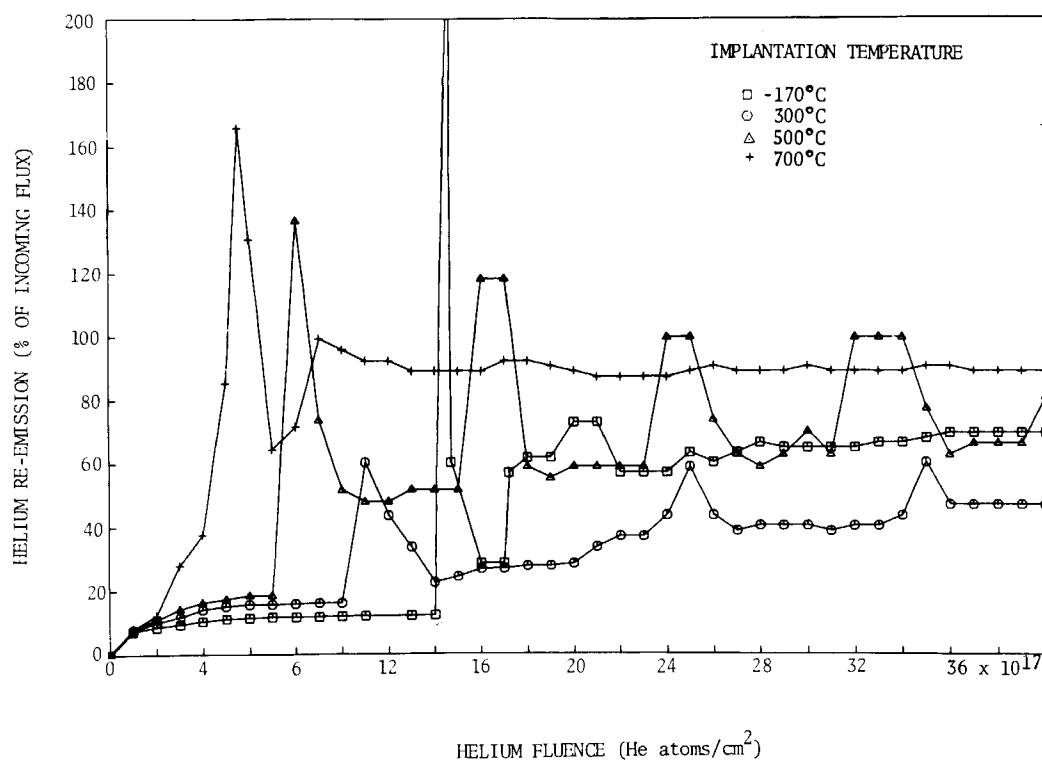
HELIUM FLUENCE (He atoms/cm^2)

Fig. 1. Helium re-emission during implantation as a function of helium fluence in 316 stainless steel at four different implantation temperatures.

partial pressure measurement in the target chamber from the main vacuum system of the accelerator.

Absolute calibration of the helium spectrometer was performed dynamically, using two independent methods. In one method a calibrated He mixture was admitted to the target chamber and the pump-out rate determined; the second method utilized a precalibrated He leak. The two methods were found to agree to within 5%. A further check on the He re-emission measurements was made by comparing the integrated dose, the He remaining in the sample after implantation, and the numerical integral of the re-emission curve. The results are discussed below. All implantations were conducted with a helium ion flux of 6.25 X 10^{13} atoms/sec at 300 keV with a helium background of ~ 2 X 10^{12} atoms/sec.

The results of a series of re-emission measurements at different temperatures, representative of the full range investigated, are shown in fig. 1. Additional runs were done at different temperatures to further delineate the temperature dependence discussed below.

In each case the re-emission in percent of incoming flux (6.25 X 10^{13} atoms/sec) is plotted as a function of accumulated dose. A number of observations can be made from these data. In every case an abrupt change in the re-emission rate occurs after a certain dose is attained. This critical dose decreases with increasing temperature; at an implantation temperature of 700°C this dose is ~ 4 X 10^{17} He atoms/cm^2 whereas at −170°C it is ~ 14 X 10^{17} He atoms/cm^2. The sudden onset of re-emission, with a peak value often well in excess of 100%, occurs at nearly the same dose as that at which surface deformation is observed optically. It is followed by a decrease to a steady state value which is also temperature-dependent. At 700°C the steady state value is nearly constant at approximately 90% of the incoming flux. At −170°C, after the initial transient behavior in the re-emission rate (between 14 and 22 X 10^{17} He atoms/cm^2), the steady state value is approximately 60% of the incoming flux.
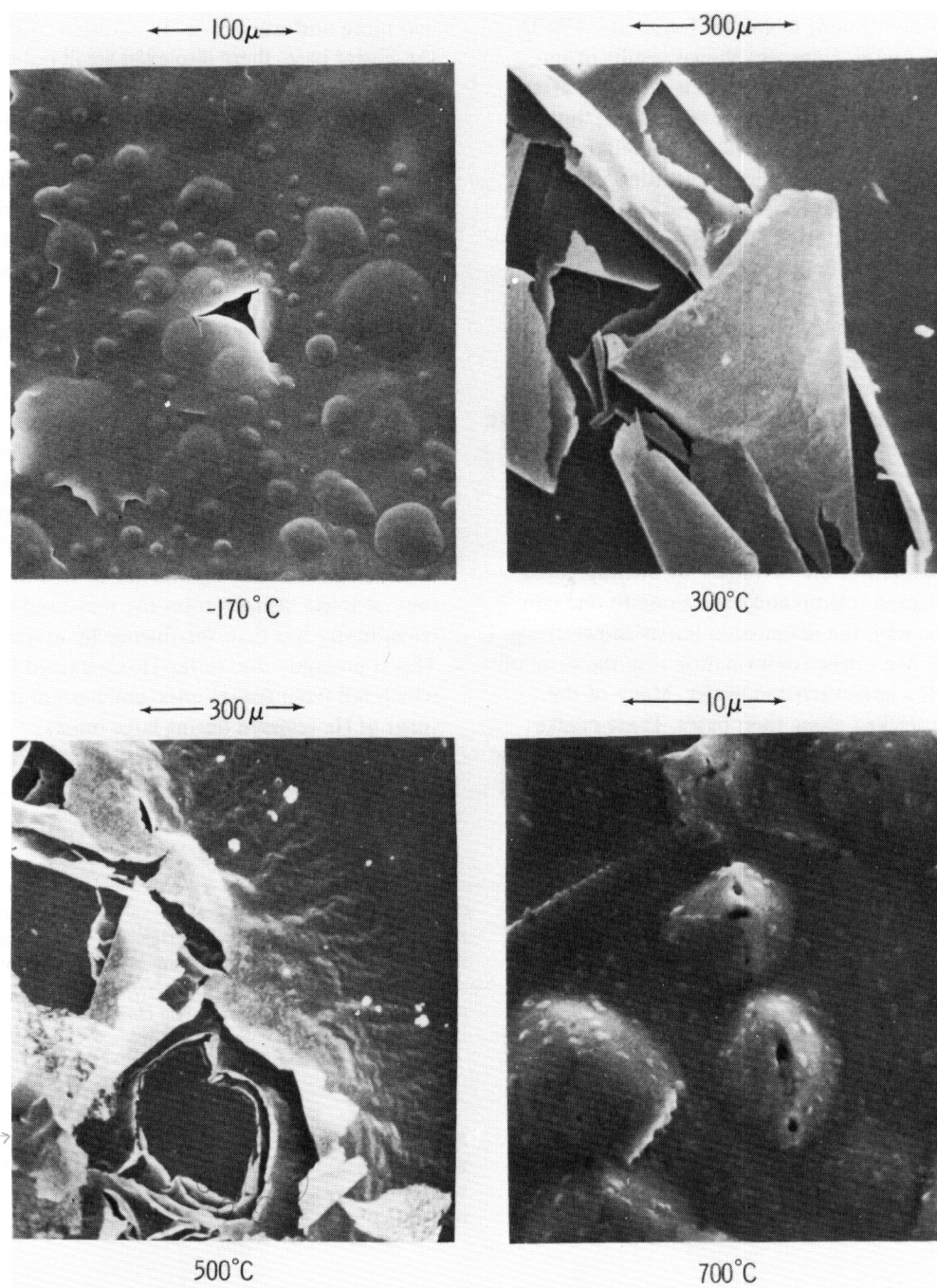
The re-emission behavior at intermediate temper-

Fig. 2. Scanning electron micrographs of 316 stainless steel samples which have been implanted to a dose of 4×10^{18} He atoms/cm^2 at the indicated temperatures. The helium re-emission data of these samples is shown in fig. 1.

atures is quite different from that found at $-170°C$ and $+700°C$. In fig. 1 are also shown results of implantation at $300°C$ and $500°C$. It is seen that after the critical dose is reached and a re-emission 'burst' occurs, the re-emission rate returns to a relatively low value. Helium again accumulates, resulting in the periodic (in dose) re-emission behavior seen in fig. 1. Optical observation during implantation indicates that the re-emission bursts are related to large scale flaking of sample surface.

The corresponding scanning electron micrographs after implantations to fluences of 4×10^{18} He atoms/cm^2 at the indicated temperatures are shown in fig. 2. The magnifications are not the same, but were chosen to illustrate different sized features. At $300°C$ and $500°C$ large scale flaking or complete exfoliation of the surface has taken place. In fact, the number of exfoliated layers (three at $300°C$ and four at $500°C$) are only apparent at the boundary of the implanted and unimplanted regions and have a one-to-one correspondence with the re-emission bursts shown in fig. 1. At $-170°C$, the surface deformation is in the form of blisters with a large variation in size. Many of the blisters are cracked along their bases. These cracks are believed to account for most of the He release. The blisters formed during $700°C$ implantation are smaller

and more uniform in size. In addition to cracks along the blister base, there also exist small holes at the top of many blisters where He has been released. The small light spots were determined to be the carbide precipitates referred to earlier. After implantation at $500°C$ these precipitates were found to be larger in the implanted region than in the unimplanted region. The onset of mobility of implantation-produced defects such as vacancies may account for the enhancement of precipitation above $500°C$.

As mentioned earlier, the total He fluence (4×10^{18} He atoms/cm^2) should be equal to the sum of the numerically integrated He re-emission curves of fig. 1 and the amount of He remaining in the samples after the experiment. The latter was measured by melting the samples in a furnace connected to the helium mass spectrometer. For the high-temperature implantation, the measured integrated quantity of helium and the remainder agreed with the fluence to within $\pm 6\%$. However, at lower temperatures the measured amount was consistently less than the fluence by as much as 20%. This is probably due to the He contained in flakes which fell from the samples, and inaccurate measurement of He released during large bursts.

Clearly the surface deformation and concomitant gas release behavior during implantation are related to

Table 1

Implantation [a] temperature region (°C)	Surface deformation	Re-emission critical dose (He atoms/cm^2)	Characteristic re-emission rate % of incoming flux	Suggested He clustering mechanism	Dominant He release mechanism
Low ($\lesssim -50°C$)	Mostly blisters	14×10^{17}	$\sim 60\%$	Percolative clustering and/or short-range He migration	Blister cracking
Medium ($\sim -50°C$ to $500°C$)	Flaking	7 to 14×10^{17}	Periodic large bursts between bursts, the rate is $\sim (30-50\%)$	Divacancy-assisted long-range He migration	Exfoliation
High $\gtrsim 600°C$	Blisters	4 to 7×10^{17}	$\sim (70-90\%)$	Vacancy-assisted bubble formation and migration	Blister cracking; some bubble migration to surface

[a] Additional runs were done to further delineate the temperature region.

gas and intrinsic defect mobilities. The main charac-
teristics of the release behavior and surface deformation
in three main temperature regions are summarized in
table 1. The temperature boundaries between the low
and medium region defined by the onset of flaking
(−50°C) are not as well defined as the reappearance of
blisters between 600 and 700°C. Also listed in the
table are possible mechanisms for the clustering pro-
cesses. In the low-temperature region the dominant
He cluster formation mechanism giving rise to blisters
is either percolative clustering [5] or short range He
migration [6]. These mechanisms have been discussed
in ref. [5]. In the intermediate temperature region a
continuous gas-filled region is formed during im-
plantation near the end of the range of the 300 keV
He atoms. When the gas pressure is sufficiently high to
overcome the strength of the material, exfoliation
occurs. This process repeats itself with a characteristic
periodicity in He dose. The formation of continuous
gas release at a certain implantation temperature implies
an increased He mobility. This may be due to the onset
of mobility of a vacancy-type defect, causing radiation-
enhanced diffusion of the He atoms. Purely on the
basis of the temperature ($\simeq$ 50°C) at which this occurs
it is suggested that divacancies may be responsible
for this radiation-enhanced effect. At temperatures
above 600°C the re-occurrence of blister formation
may be due to the 'classical' formation of He bubbles
and an agglomeration mechanism involving single
vacancy migration.

In summary, it has been shown that the nature of
He re-emission during implantation is closely related
to surface deformation at all temperatures investigated.
Both the re-emission and surface deformation are
strongly dependent on the implantation temperature.
These temperature-dependent effects are explained
by a qualitative model based on radiation enhanced
He diffusion.

Acknowledgements

References

[1] M. Kaminsky and S.K. Das, Appl. Phys. Lett. 21 (1972)
443.
[2] S.K. Erents and G.M. McCracken, Proc. Int. Conf. on
Ion-Surface Interaction Sputtering and Related Phenomena
(Garching, 1972).
[3] W. Bauer and D. Morse, J. Nucl. Mater. 44 (1972) 337.
[4] W. Bauer and G.J. Thomas, J. Nucl. Mater. 42 (1972) 96.
[5] G.J. Thomas and W. Bauer, Radiation Effects, to be
published.
[6] W.D. Wilson and R. Johnson, Rare Gases in Metals, Proc.
of Int. Conf. on Simulation of Lattice Defects with In-
teratomic Potentials (British Columbia, Canada, June
14–19, 1971).

Appendix E

Reproduced, herein is a corrected copy of a reply from

Dr. Kaminsky to Allan T. Mense concerning an explaination of the

"chuck" emission process from 14 MeV neutrons on Nb.   Also present

is a reproduction of Dr. Kaminsky's recent Phys. Rev. Letter of

18 March 1974.

ARGONNE NATIONAL LABORATORY

February 6, 1974

Dr. Allan T. Mense
Fusion Design Group
Nuclear Engineering Department
University of Wisconsin
1500 Johnson Drive
Madison, Wisconsin 53706

Dear Dr. Mense:

This is a brief reply to your review of the Philadelphia conference raising the question about the energetics of the chunk emission process. Our experimental results indicate the following. The number of chunks emitted per unit area (cm^2) decreases from $\sim 1,000$ for a cold rolled poly Nb surface with a microfinish of $5\mu m$, to ~ 200 for an annealed poly Nb surface with a microfinish of $2\mu m$, to ~ 70 for an annealed poly Nb surface with a microfinish of $0.5\mu m$. Furthermore, the chunk deposits are not uniformly distributed over the collector area but are clustered along certain streaks or appear in certain patches. The direction of the streaks appears to be identical with the direction of cold-rolling of the niobium sample and is not related to any microstructure of the collector surface.

These observations suggest the following chunk emission process. In any consideration of the energetics of the chunk emission process it is necessary to take into account not only the energy deposited by the energetic recoil atoms (e.g. $\overline{E} = 180$ keV, $E_{max} = 600$ keV for Nb recoil atoms) in small volumes (e.g. assume spherical volume with r = 500 Å [fraction of range of energetic recoil atoms]) in near surface regions but also the stored energy in the crystal due to forming processes (e.g. cold rolling, leading to $\sim 10^8$ ergs cm^{-3} or $\sim 10^{-4}$ ergs per 10^{-12} cm^3 chunk volume). The release of part of the stored energy can be triggered by the temperature – and the displacement-spike caused by the energy deposition of the energetic recoil atom. (Annealing of the cold rolled targets will also cause a partial release of stored energy.) Furthermore, it is very important to take the microstructure of the surface (e.g. surface roughness - the existence of small protrusions, hillocks, microcracks, etc.) into account. For example, for a protrusion which is bound at its base to the substrate lattice by only a small number of lattice atoms (say 10^5 to 10^6 atoms per bonding area) a relatively small amount of the deposited and stored energy is required (assume 0.1 eV per bond) to break the bonds. Similarly, microcracks can grow and intersect and cause the loosening of chunks in surface regions.
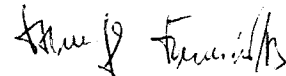
- 2 -

Now, from the mass of our chunks (10^{-10} — 10^{-11} grams) and from the estimated velocity range of our chunks ($\overline{V} \lesssim 10$ cm sec^{-1}) [inferred from the position of the impact points of the chunks on the collector relative to the assumed target position with the additional assumption that the trajectory is influenced by gravity], the kinetic energy of the chunks can vary from $\sim 10^{-8}$ to $\sim 10^{-11}$ ergs. This would correspond to only 1% to 0.01% of the energy deposited by a 600 keV recoiling Nb atom (stored energy is not even taken into account).

Experiments are in progress to investigate the neutron sputtering process in more detail.

In reading your summary I find that I would like to comment on several other parts of your draft. I will send you my comments plus the pictures you requested in a separate letter.

Sincerely yours,

Manfred Kaminsky
Physics Division

cc: Dr. Klaus M. Zwilsky
Dr. G. L. Kulcinski

(1957).

[4]For AgI, for example, see K. H. Lieser, Z. Phys. Chem. 9, 302 (1956).

[5]A. B. Lidiard, *Encyclopedia of Physics*, edited by S. Flügge (Springer, Berlin, 1957), Vol. 20, pp. 258–261.

[6]S. Strässler and C. Kittel, Phys. Rev. 139, A758 (1965).

[7]It follows from Eq. (7) that if $\epsilon_0/\lambda > g/(1+g)$ the value of $\rho(T_c)$ will exceed the infinite-temperature value of ρ, $\rho_\infty = g/(1+g)$, so that $d\rho/dT$ will be < 0 above T_c. Below T_c, $d\rho/dT$ will always be > 0. For such a "supertransition" (Ref. 6), it follows from Eq. (9) that the volume-expansion coefficient $\alpha_p(T)$ will undergo a sign change at T_c. Note that the transitions shown in Fig. 1 are "supertransitions."

[8]B. Huberman (to be published) has recently suggested that it is the effective attraction between an interstitial cation and the vacancy it has left behind that is the basic interaction responsible for the phase transition. It is difficult to find physical justification for Huberman's argument.

[9]W. T. Richard and G. Jones, J. Amer. Chem. Soc. 31, 158 (1909).

[10]S. Hoshino, J. Phys. Soc. Jap. 12, 315 (1957).

[11]H. Hoshino and M. Shimoji, J. Phys. Chem. Solids 33, 2303 (1972).

[12]Note that if the vibrational contribution to $S(\rho)$ is of the form $S(\rho)_{\mathrm{vib}} = k_B \rho \ln g_{\mathrm{vib}}$, where g_{vib} denotes a characteristic constant, it follows from Eq. (3) that the effective degeneracy factor appearing in our model will be just $g_{\mathrm{eff}} = g_{\mathrm{vib}} g$.

Particle Release from Niobium Irradiated with 14-MeV Neutrons*

M. Kaminsky, J. H. Peavey, and S. K. Das

Argonne National Laboratory, Argonne, Illinois 60439

The particle release from cold-rolled niobium surfaces under 14-MeV–neutron impact to a total dose of 4.6×10^{15} neutrons/cm^2 was investigated under ultrahigh-vacuum conditions and at ambient temperature. The type and amount of material released and deposited on a substrate surface was determined independently by four analytical techniques. Surprisingly, there were two types of deposits—one in the form of large chunks, the other a more even layer covering the surface. The chunk emission cannot be explained by existing neutron-sputtering theories.

It has been suggested[1-3] that the bombardment of the first wall of fusion reactors by MeV neutrons may lead to both serious wall erosion and plasma contamination. Unfortunately, the experimental information available on particle release by MeV-neutron impact on solids is very scarce and contradictory (for reviews, see Refs. 1–3). For example, for monocrystalline gold irradiated with 14-MeV neutrons, the particle release yield $S = 3 \times 10^{-3}$ atom/neutron was reported.[4] However, for iron irradiated with neutrons of a softer energy spectrum (from a fission reactor), $S = (5.7 \pm 0.8) \times 10^{-3}$ atom/neutron was reported.[5] A theoretical estimate of S for niobium irradiated with 14-MeV neutrons by one of us (M.K.) yielded $S \approx 6 \times 10^{-5}$ atom/neutron—a value which was approximately 2 orders of magnitude smaller than the above-mentioned experimental value for gold. More recently Behrisch[6] and Behrisch and Vernickel[7] estimated a yield value for 14-MeV–neutron–bombarded niobium that was only about a quarter of that of Kaminsky. On the basis of such an estimated value, these authors con-

cluded that neutron sputtering would have a negligible effect on wall erosion and plasma contamination during the operation of a fusion reactor. In view of the great discrepancy between the theoretical estimates and the available experimental results, it seemed imperative to conduct new experiments under controlled conditions.

The present experiments were undertaken to provide information on the erosion of surfaces of cold-rolled polycrystalline niobium under 14-MeV–neutron impact in an ultrahigh-vacuum environment. The Lawrence Livermore Laboratory's rotating-target neutron source[8-10] was used in conjunction with an insulated-core-transformer accelerator. The total neutron emission rate over the entire 4π solid angle of a fresh neutron-source target was about 3×10^{12} neutrons/sec. The irradiation run was monitored with two proton-recoil detectors.[9,10] The drift in counting efficiency of each recoil detector is thought to be less than 5%.[11] The total dose was calibrated independently by activation analyses,[10] for example, by use of the reaction $^{93}\mathrm{Nb}(n, 2n)^{92}\mathrm{Nb}$. The

absolute accuracy in the determination of the average dose the sample received was estimated to be ±7.5%. The targets were mounted in a train assembly containing 17 targets and were placed inside a vacuum chamber. The distance between the neutron-source disk and the front face of the first target, a monocrystalline Si(111) disk approximately 2.5 cm in diameter and 0.5 cm thick, was ~1.75 cm. A space of 0.28 cm separated this disk from the second target—a circular cold-rolled polycrystalline niobium foil with a diameter of approximately 2.5 cm and a thickness of 0.013 cm. The third target, again a monocrystalline Si(111) disk with dimensions similar to those of target No. 1, was spaced ~0.28 cm from the second target. The center of the neutron-source disk and the center of each of the three target disks were on the same axis.

The undoped, optical-grade monocrystalline Si(111) disks (obtained from the Materials Research Corporation) had a purity of 99.999%. They were first mechanically and then chemically polished and had a surface microfinish of ~0.03 μm. The cold-rolled polycrystalline niobium sample was obtained from Materials Research Corporation (Marz grade). It was mechanically polished and lightly electropolished[12] and had an average surface microfinish of ~5 μm (a coarse mirror finish with some scratch traces still present). The average grain size of the cold-rolled niobium was 3–10 μm. The target chamber was evacuated with sorption pumps and subsequently with a combination titanium-sublimation–ion pump. At the beginning of the neutron irradiation run, the pressure in the chamber was ~1.5×10^{-9} Torr, and it dropped to ~4×10^{-10} Torr towards the end of the ~54-h irradiation run. The total 14-MeV–neutron dose on the niobium foil was estimated from the total number of counts of the proton-recoil counters (with the appropriate corrections for the relative positions of source, counter, and target, for the effective neutron absorption length, and for the neutron flux peaking in the forward direction). The estimated dose was ~4.6×10^{15} neutrons/cm^2, and the average dose rate was ~2.4×10^{10} neutrons cm^{-2} sec^{-1}. During the irradiation the targets were at ambient temperature (estimated to be near room temperature). The irradiated targets were transported under ultrahigh-vacuum conditions (~1×10^{-9} Torr) from Lawrence Livermore Laboratory to Argonne National Laboratory for analysis.

To determine the type and amount of the mate-

rials released from the surface of one sample (e.g., niobium target No. 2) and deposited on the surface of the one facing it [e.g., Si(111) target No. 1] the analytical techniques used were Rutherford backscattering (using a 750-keV ^{4}He$^+$ ion beam from a 2-MeV Van de Graaff accelerator), Auger spectroscopy, ion-microprobe microanalysis (an Applied Research Laboratories ion microprobe), and scanning electron microscopy (a Cambridge Stereoscan Mark IIA) in conjunction with an energy-dispersive x-ray spectrometer. The amount of deposited material could be estimated quantitatively by using calibration standards prepared by vapor deposition. For the niobium deposits, the detection sensitivities [expressed as fractions of a monolayer (ML) of niobium deposited on silicon substrate] of three of the analytical techniques (in order of decreasing values) were, for Rutherford backscattering, ~0.0005 ML; for ion microprobe, ~0.001 ML; and for Auger spectroscopy, ~0.01 ML. The scanning electron microscope together with an energy-dispersive x-ray spectrometer was also used to identify the deposits. A metallograph was used for visual inspection of the irradiated targets. To test contamination buildup during the period of storage, unirradiated targets were kept in the ultrahigh-vacuum storage chamber. No significant contamination buildup could be detected.

An examination of the surface of Si(111) target No. 1 which faced the cold-rolled polycrystalline niobium target revealed the surprising result that the niobium deposits appeared in two forms. One form covered the substrate surface as a fractional atomic layer with an estimated "average" coverage degree of ~0.026 ML. The other form appeared as chunks of various irregular shapes as illustrated in Fig. 1. The optical micrograph in Fig. 1(a) shows some of the chunks. The secondary-ion (^{93}Nb$^+$) micrograph shown in Fig. 1(b) was obtained for the same area as in Fig. 1(a); it confirmed that the chunks were niobium. The larger fraction of the chunks (approximately $\frac{4}{5}$ of the total deposits) appears to be roughly spherical in shape [e.g., chunk No. 1 in Figs. 1(c) and 1(d)], while the smaller fraction (approximately $\frac{1}{5}$ of the total deposits) appears to be more cylindrical in shape [e.g., chunk No. 3 in Fig. 1(c)]. Some of the more cylindrically shaped chunks have their long axes nearly normal to the surface of the Si(111) substrate. Many of the chunks show microprotrusions in certain regions.

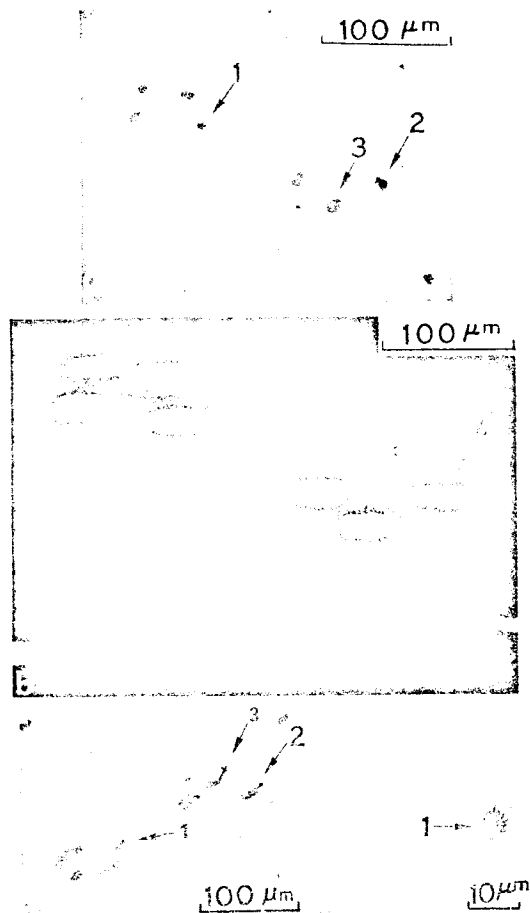So far the size distribution of the chucks has

FIG. 1. Niobium deposited on a silicon (111) substrate when a niobium target at ambient temperature (estimated to be near room temperature) was irradiated with 14-MeV neutrons to a total dose of 4.6×10^{15} neutrons/cm^2. (a) Optical micrograph of niobium chunks deposited on a Si(111) surface. (b) Secondary-ion (^{93}Nb$^+$) micrograph of the same area as in (a). (c) Scanning electron micrograph (backscattered electron image) of the same area as in (a), showing the size and shape of the deposited chunks of Nb. (d) An enlarged view of a roughly spherical chunk, No. 1, shown in (c).

been only crudely estimated from the enlarged scanning electron micrographs. Since the chunks were irregular in shape, the "average" diameter of either a roughly spherical or a cylindrically shaped chunk was defined as the diameter of a circle whose area is equal to that of the projection of the chunk onto the surface plane. For the cylindrically shaped chunks, the "average" diameter ranged from about 0.5 to 5 μm, while the lengths of the cylinders ranged from about 3 to 15 μm. A majority of these chunks have a volume

of $\sim 4 \times 10^{-11}$ cm^3, which corresponds to $\sim 2 \times 10^{12}$ atoms/chunk. The spherically shaped chunks had "average" diameters ranging from approximately 1 to 5 μm. A majority of these chunks have a volume of about 1×10^{-11} cm^3, which corresponds to about 5×10^{11} atoms/chunk. For both types of chunks, the distribution over the irradiated substrate surface area is nonuniform. The estimates given above are very crude and work is in progress to improve the accuracy of these estimates.

An investigation of the Si(111) surface of target No. 3 which faced the backside of the polycrystalline niobium target No. 2 revealed niobium chunk deposits similar to those reported above for target No. 1. The surface of Si(111) target No. 1 which faced the stainless steel flange revealed chunk deposits of stainless steel. The surface of cold-rolled polycrystalline niobium which faced the Si(111) target No. 1 revealed chunk deposits of silicon.

By ion milling the chunks to about $\frac{1}{10}$ of the original size by using the ion microprobe with 20-keV O$^-$ ions, it was determined that the chunks consisted of niobium and that they did not contain contaminants to any significant degree. The binding of the niobium chunks to the Si(111) substrate appeared to be rather strong since the chunks could not be readily scrapped off mechanically, or burned off by the high flux (~ 3 mA/cm^2) of 20-keV oxygen ions. In a second irradiation run the cold-rolled niobium foil was replaced by an annealed one. A preliminary examination of the deposits revealed again niobium chunks but their number was smaller than observed for the cold-rolled foil.

A crude estimate based on the assumption that the niobium deposits were smeared out evenly over the Si(111) substrate No. 1 yielded an equivalent surface-coverage degree of 0.86 ML for all types of niobium deposits. For Si(111) target No. 3 the average surface-coverage degree of the niobium deposit was found to be $\sim 20\%$ higher than the value quoted above for target No. 1. For the cold-rolled polycrystalline niobium sample, the fractional "atomic" layer deposit alone gives a yield value of $S = (8.7 \pm 3.0) \times 10^{-3}$ niobium atom per neutron. Considering both the chunk and the atomic layer deposits, a total yield $S = 0.25 \pm 0.10$ niobium atom per neutron is obtained.

On the basis of the two types of deposits observed, the authors speculate that target particle emission via momentum transfer from collision cascades will contribute only partially to the fractional atomic layer deposit but will not con-

tribute significantly to the chunk deposits. The mechanism for the emission of chunks is not clearly understood. A possible mechanism for the ejection of chunks could be related to the energy deposited by a 14-MeV neutron interacting with niobium lattice atoms in the near-surface region via elastic and inelastic collisions. (The calculated mean and maximum energies for primary knock-on niobium atoms are 181 and 600 keV, respectively.[1]) This deposited energy can lead to localized thermal and ionization (electron) spikes which in turn may cause the generation of shock waves. The interference of such shock waves in a small volume in the near-surface region in which the stored energy is very high (as a result of cold working) may set up stresses large enough to release energy by initiating submicroscopic cracks or by propagating already existing microcracks and cause the emission of chunks. However, one cannot exclude the possibility that other mechanisms may contribute to or dominate the chunk-ejection process.

The yield $S = 0.25 \pm 0.1$ niobium atom/neutron obtained for cold-rolled polycrystalline niobium with a surface finish of only ~ 5 μm at near room temperature leads to an annual erosion rate of 0.6 ± 0.3 mm/yr for a neutron flux of 4×10^{14} neutrons cm^{-2} sec^{-1}. If the erosion rates for a fusion reactor wall at operating temperature are similar to those obtained here, then erosion by neutron impact cannot be neglected, contrary to the conclusion by others.[6,7]

*Work performed under the auspices of the U. S. Atomic Energy Commission.

[1]M. Kaminsky, IEEE Trans. Nucl. Sci. 18, 208 (1971).

[2]M. Kaminsky, in *Proceedings of the International Working Session on Fusion Reactor Technology, Oak Ridge National Laboratory, Oak Ridge, Tennessee, 1971*, CONF-719624 (U.S. Atomic Energy Commission, Oak Ridge, Tenn., 1971), pp. 86 ff.

[3]M. Kaminsky, in *Proceedings of the Seventh Symposium on Fusion Technology, Grenoble, France, 1972* (Commission of the European Communities, Luxembourg, 1972), p. 41.

[4]R. Garber, G. Doyla, V. Kolyada, A. Modlin, and I. Federenko, Zh. Eksp. Teor. Fiz. Pis'ma Red. 7, 375 (1968) [JETP Lett. 7, 296 (1968)].

[5]T. S. Baer and J. N. Anno, J. Appl. Phys. 43, 2453 (1972).

[6]R. Behrisch, Nucl. Fusion 12, 695 (1972).

[7]R. Behrisch and H. Vernickel, see Ref. 3, p. 27.

[8]R. Booth and H. H. Barschall, Nucl. Instrum. Methods 99, 1 (1972).

[9]E. Goldberg, R. Griffith, and L. Logan, Lawrence Livermore Laboratory Report No. UCRL-51317, 1972 (unpublished).

[10]R. A. van Konynenburg, Lawrence Livermore Laboratory Report No. UCRL-51393, 1973 (unpublished).

[11]R. Booth, private communication.

[12]S. K. Das and M. Kaminsky, J. Appl. Phys. 44, 25 (1973).

Appendix F

Reproduced here is a letter from Ralph Moir on his ideas concerning toroidal vs. Poloidal divertors on Tokamak reactors.

LAWRENCE LIVERMORE LABORATORY

March 27, 1974

Mr. Allan Mense
1500 Johnson Drive
University of Wisconsin
Madison, Wisconsin   53706

Dear Allan:

My comments at the impurity meeting last November were more or less as follows: "Mirror reactors as we see them now are not bothered by impurities because the plasma potential is strongly positive thus repelling impurity ions that try to enter along the field lines and quickly ejecting impurities that try to enter across the field lines. Plasma that leaks out of the machine enters the direct converter where pumping is provided and where the plasma density is so low in the direct converter that the mean free path for ionization is bigger than the characteristic dimensions.

For toroidal machines the opposite situation is true in that the plasma potential is negative with respect to the separatrix flux surface. Now then if the potential on the separatrix can be made positive with respect to the walls then from the separatrix on out the machine looks like a mirror machine. This potential shape can be achieved if the field line length from the separatrix to the disposal region is not too long. These field lines are quite long for a Poloridel Diverter but relatively short for a toroidal diverter as shown in figure 1. Further, if the field strength drops as in the toroidal divertor then there will be a strong outward magnetic gradient force on both ions and electrons that will generate a plasma flow that will sweep impurities out of the machine.

A toroidal diverter would introduce azimuthal assymetry but several could be placed periodically around the machine. One also might expect trapped particle modes to be enhanced.

A toroidal diverter would naturally allow a large jumping region and in the future, direct conversion could be adapted as shown in figure 2 (especially useful for a D-D-H_e^3-T cycle).

I think the toroidal diverters should be investigated for toroidal confinement concepts like the Tokamak."

Sincerely,
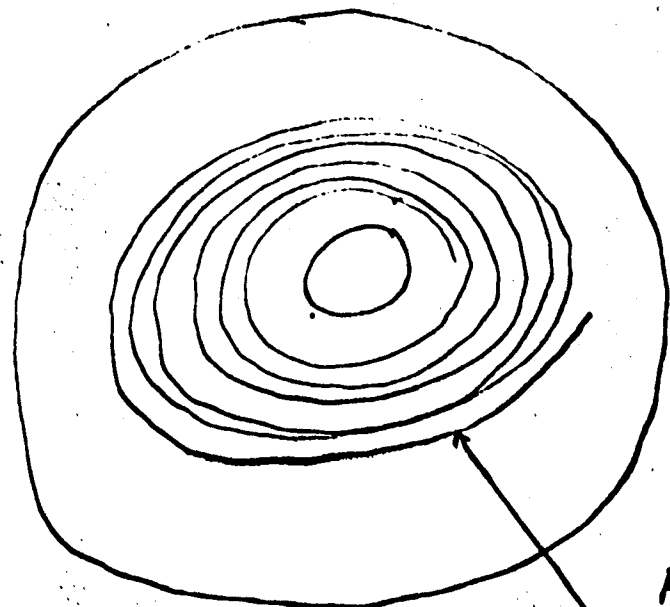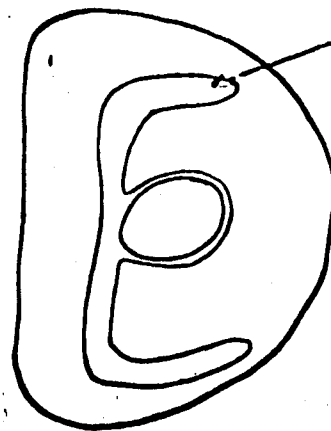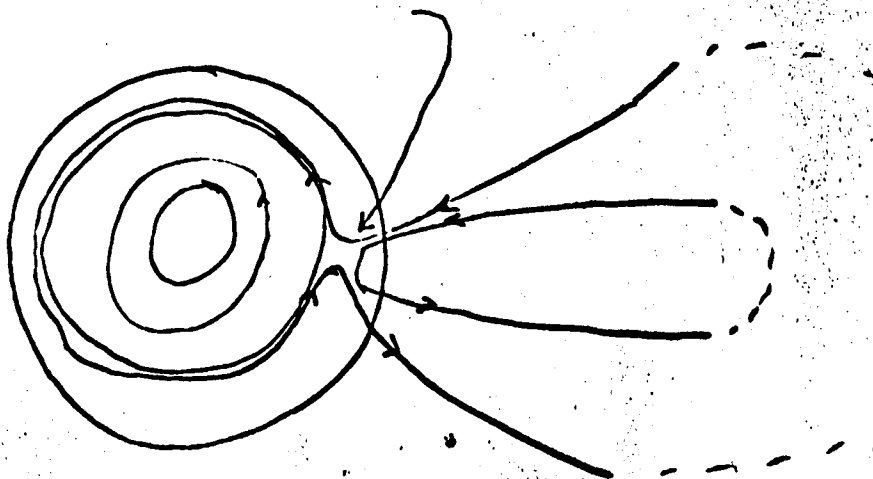
Ralph W. Moir

RWM:jd

Enclosures: 2

RESTRICTED PUMPING

POLOIDAL DIVERTER

TOP VIEW

LONG PATH LENGTH

SHORT PATH LENGTH OUT

NOZZLE

LARGE VOLUME PUMPING

TOP VIEW

TOROIDAL DIVERTER

FIG 1

Detail B

Detail A

Reactor

Diverter

Expander

Direct energy converter
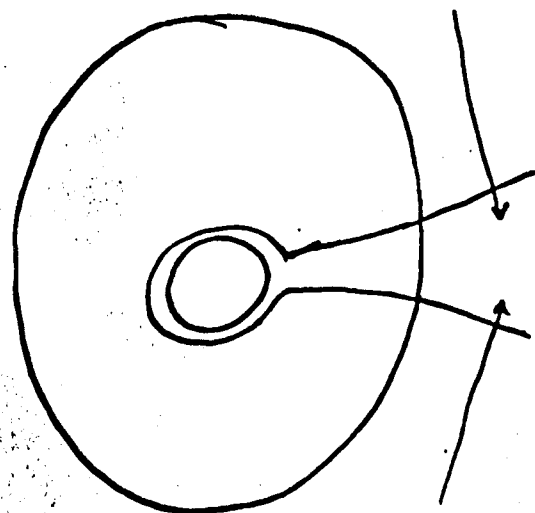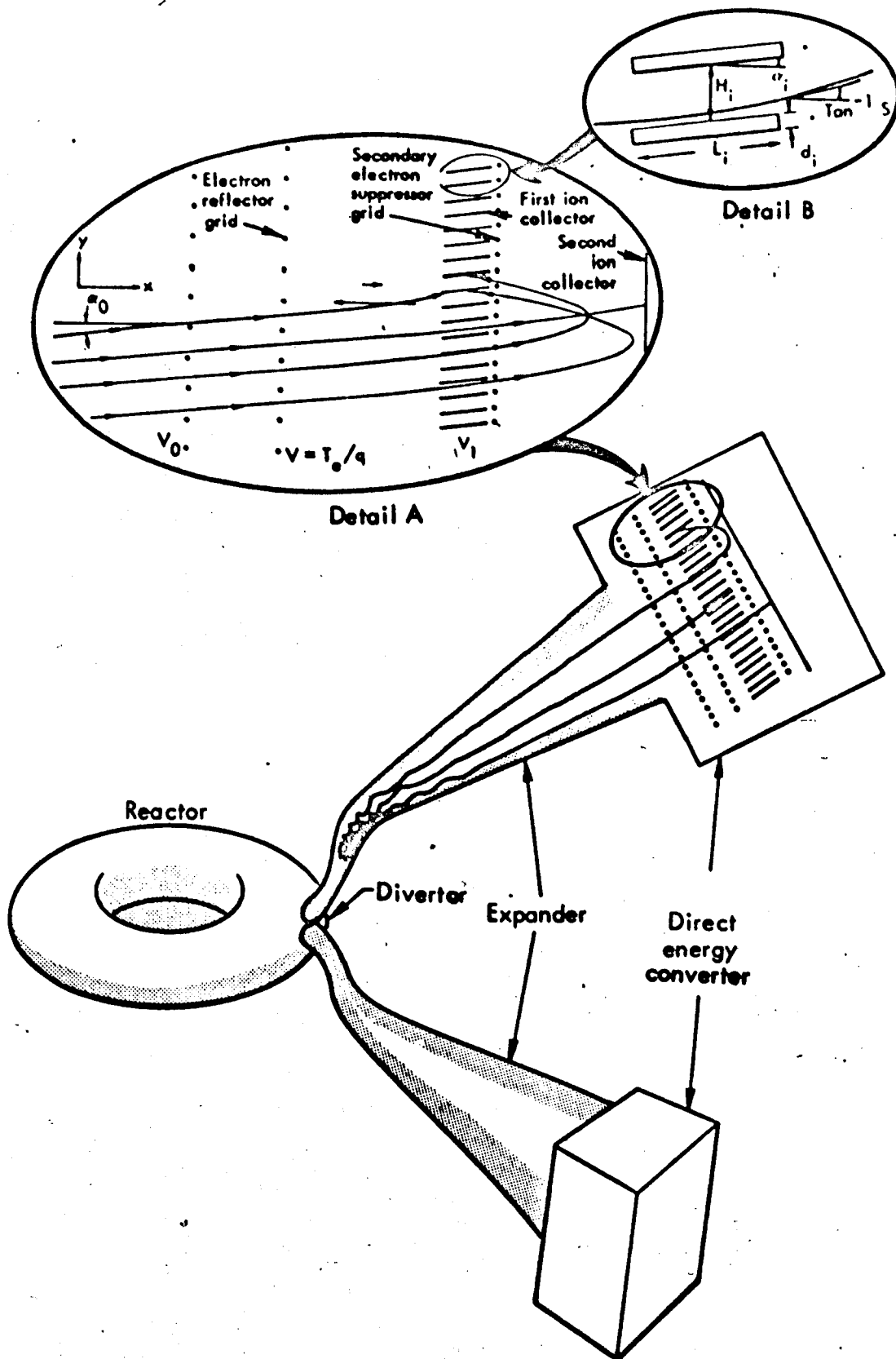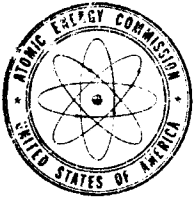
HS 701

Moir - Fig. 1

Appendix G

Reproduced here is the original letter from Wm. C. Gough and
F. Robert Scott concerning the impurity control meeting and its
objectives. I am not sure we addressed all of these questions.

UNITED STATES
ATOMIC ENERGY COMMISSION
WASHINGTON, D.C. 20545

Those Listed Below

Subject: INFORMAL MEETING ON IMPURITY CONTROL IN TOROIDAL SYSTEMS

Gentlemen:

The question of impurity control in toroidal systems becomes increas-ingly important as we plan for the next generation of Tokamak systems and extrapolate to fusion reactors. The problem is interdisplinary and requires a close working relationship among plasma physicists, surface physicists, and design engineers. Within the CTR community individuals with varying backgrounds have been giving serious thought to the impurity control question (including "divertor" development). These include plasma physicists concerned with the next generation of confinement experiments; the surface physicists, chemists and engineers concerned with photon, particle, and vacuum problems of fusion reactors; and the engineers and physicists doing conceptual designs of future experiments and fusion reactors.

These diverse groups have not interacted frequently. The American Physical Society meeting in Philadelphia provides us with an oppor-tunity to hold an informal get-together so that these individuals may meet and discuss their views on the nature of the toroidal system impurity control problem and the various options available to us.

Because of your work in these areas, you are invited to participate in what we hope will be an open and frank exchange of knowledge and ideas on the subject of impurity control in toroidal systems. We will meet in the Valley Forge Room of the Ben Franklin Hotel at 4:30 p.m. on October 30, 1973. In order to obtain a free room and to use our time effectively, we plan to eat dinner during the meeting. The meal will cost approximately $10 per person, including tip and taxes.

To stimulate discussion we have attached a list of thoughts and questions we have in this area. Although these questions certainly are not all inclusive, we suggest that you come prepared to discuss those rele-vant to your interests. You may even wish to have written material for distribution at the meeting. We look forward to seeing you. A viewgraph and blackboard will be available.

Sincerely,

William C. Gough

F. Robert Scott
Division of Controlled
Thermonuclear Research

Enclosure (As stated)
Addressees:
  See attached list

IMPURITY CONTROL IN TOROIDAL SYSTEMS

The substance of the meeting can be divided into three general, but related areas. The plasma physics of the boundary, the physical demands placed on the material walls, and the engineering constraints on the system. These areas are explored in the form of questions which may have explicit answers, may require discussion to qualify or may need further work.

1) What are the physical parameters of the boundary for each of our presently operating and planned experimental tokamak devices, and our future reactor design?

2) What is the present state of the art on divertor operation?

3) What effect does the plasma in the divertor region have on the stability and transport processes in the plasma core as well as the plasma boundary? For example, what is its effect on the boundary "skin effect"?

4) With the specified physical parameters of our present and future tokamaks what are the anticipated first wall problems? What should be the criteria for selection of materials? What do we know about the conditioning of surfaces?

5) At what point in our present and projected program will our boundary problems dominate the plasma characteristics?

6) No divertors have been used with a high energy density plasma under the continuous operation required for advanced fusion systems. What steps should be taken to increase our confidence that divertors will work? What alternative do we have?

7) Considering the overall demands on a divertor and the stability and equilibrium requirements of the tokamak containment system, what are the anticipated advantages of poloidal divertors over toroidal divertors? What experience do we have which leads to confidence in a poloidal divertor?

8) In considering alternatives to divertors in the impurity control problems of tokamaks, what information is available to evaluate options such as gas blankets, limiters, pulsed operation, or a torsatron?

9) With regard to impurity control, what are the relevant physical phenomena that occur on a material wall exposed to the environment of our present and projected fusion devices? Which of these phenomena appear to be controllable by presently known methods? Which need further work?

10) What are the anticipated engineering limitations in impurity control we will face as we approach larger systems.